Assessment of the impacts of cloud chemistry on surface SO$_2$ and sulfate levels in typical regions of China

Jianyan Lu[1], Sunling Gong[1,5]*, Jian Zhang[1], Jianmin Chen[2,3,4],   Lei Zhang[1], Chunhong Zhou[1]*

[1] State Key Laboratory of Severe Weather, Key Laboratory of Atmospheric Chemistry of CMA, Institute of Atmospheric Composition, Chinese Academy of Meteorological Sciences, Beijing 100081, China

[2] Shanghai Key Laboratory of Atmospheric Particle Pollution and Prevention (LAP3), Department of Environmental Science and Engineering, Fudan Tyndall Centre, Institute of Atmospheric Sciences, Fudan University, Shanghai, China

[3] Center for Excellence in Urban Atmospheric Environment, Institute of Urban Environment, Chinese Academy of Science, Xiamen, China

[4] Shanghai Institute of Eco-Chongming (SIEC), No.3663 Northern Zhongshan Road, Shanghai 200062, China

[5] National Observation and Research Station of Coastal Ecological Environments in Macao, Macao Environmental Research Institute, Macau University of Science and Technology, Macao SAR 999078, China

* Corresponding authors.
E-mail addresses: gongsl@cma.gov.cn (S. Gong), zhouch@cma.gov.cn (C. Zhou)

Abstract

A regional online chemical weather model WRF/ CUACE (China Meteorological Administration Unified Atmospheric Chemistry Environment) is used to assess the contributions of cloud chemistry to the SO$_2$ and sulfate levels in typical regions of China. By comparing with several time series of in-situ cloud chemical observations on Mountain Tai in Shandong Province of China, the CUACE cloud chemistry scheme is found to reasonably reproduce the observed cloud consumption of H$_2$O$_2$, O$_3$ and SO$_2$ and the production of sulfate, and consequently is used in the regional assessment for a heavy pollution episode and monthly average in December 2016. During the cloudy period in a heavy pollution episode, the sulfate production was increased by 60-95% and SO$_2$ was reduced by over 80%. The cloud chemistry mainly affects the middle and lower troposphere below 5 km as well as within the boundary

layer, and contributes significantly to the SO_2 reduction and sulfate production in east-central China. Among the four typical regions in China, the Sichuan Basin (SCB) is mostly affected by the cloud chemistry, with the average SO_2 abatement about 1.0-15.0 ppb and sulfate increase about 10.0-70.0 μg/m^3, followed by Yangtze River Delta (YRD) and southeast of North China Plain (NCP), where SO_2 abatement is about 1.0-3.0 ppb and sulfate increase is about 10.0-30.0 μg/m^3. However, the cloud chemistry contributions to the Pearl River Delta (PRD) and northwest of NCP are not significant due to lighter pollution and less water vapor than other two regions. This study provides a way to analyze the over-estimate phenomenon of SO_2 in many chemical transport models.

Keywords: SO_2, sulfate, cloud chemistry, WRF/CUACE

1 Introduction

Aerosols interact with radiation and clouds, directly or indirectly affecting the atmospheric radiation balance and precipitation, which in turn affects weather and climate (Twomey et al., 1984; Twomey, 1991; Charlson et al., 1992; Ramanathan et al., 2001; Pye et al., 2020) . Moreover, large amounts of aerosols dispersed in the atmosphere can reduce visibility and deteriorate air quality (Molina, 2002), which is harmful to human health and ecosystem (Xie et al., 2019; Sielski et al., 2021).

In addition to direct emissions, aerosols are mostly produced secondarily through the oxidation of precursor gases, and one of the important processes is the transformation in clouds. Global cloud coverage of about 21% to 95% provides an adequate environment for cloud chemistry processes (Kotarba, 2020; Ravishankara, 1997). As about 90% of the clouds formed in the atmosphere evaporate without deposition or forming the precipitation, large fractions of aerosols formed in them can then re-enter the atmosphere (Caffrey et al., 2001; Harris et al., 2013; Lelieveld et al., 1992). Globally, sulfate production from SO_2 oxidation accounts for about 80% of total sulfate, and more than half of it is produced in clouds (Hung et al., 2018; Faloona et al., 2010; Guo et al., 2012). Ge et al. (2021) found that cloud chemistry processes reduced the SO_2 concentrations by 0-50% in most of east-central China in all seasons. Li (2011) found that the average SO_4^{2-} concentration in cloud water accounted for 53.8% of the total aerosol concentration at a mountain site. Li et al. (2020) also found that cloud processes effectively

reduced atmospheric O_3 and SO_2 concentrations by an average of 19.7% and 71.2%, respectively, at Mount Tai.

Multiphase oxidation of SO_2 in aerosol particles in high humidity environment is one of the main causes of explosive growth of particulate matter in East Asia haze (Guo et al., 2014; Cheng et al., 2016; Song et al., 2019). From observations and laboratory works, four main pathways were found for this kind of oxidation of SO_2 , i.e. by H_2O_2, O_3, NO_2, and transition metal ions (TMIs) (IIbusuki and Takeuchi, 1987; Martin et al., 1991; Alexander et al., 2009; Harris et al., 2013; Cheng et al., 2016; Wang et al., 2016; Wang et al., 2021). Additional pathways of organic peroxides (ROOH) (Yao et al., 2019; Wang et al., 2019; Ye et al., 2018; Dovrou et al., 2019), photolysis products of nitrate (pNO_3^-) (Gen et al., 2019a; 2019b), and excited triplet states of photosensitizer molecules (T*) (Wang et al., 2020) have also been found recently to be important for multiphase oxidation of SO_2 during very heavy hazy days. Unfortunately there are still much uncertainties and gaps to put all of those pathways into model applications from observational and laboratory studies (Pye et al., 2020; Ravishankara, 1997; Liu et al., 2021). Several regional and global models have tried to include only two, O_3 and H_2O_2, in-cloud oxidant in cloud chemistry mechanisms (Park et al., 2003; Tie et al., 2005; Salzen et al., 2000; Chapman et al., 2009; Leighton and Ivanova, 2008; Ivanova and Leighton, 2008). A very few models can simulate the pathway of NO_2, TMIs of Fe or Mn ions (Ge et al., 2021; Binkowski and Roselle, 2003; Chang et al., 1987; Terrenoire et al., 2015; Meleux, et al., 2013).

There has been very serious air pollution in central-east China where four heavy pollution regions of North China Plain (NCP), Yangtze River Delta (YRD), Sichuan Basin (SCB) and Pearl River Delta (PRD) are located (Yao et al., 2021; Zhang et al., 2012). Although many global and regional models have contained sulfate formation mechanisms by cloud chemistry, few models have assessed its contribution, especially the lack of detailed assessment of regional cloud chemistry on sulfate and SO_2 in China. Some models have reported that they fail to reproduce SO_2 and sulfate, particularly underestimating sulfate and overestimating SO_2 over China (Buchard et al., 2014; Hong et al., 2017a; Wei et al., 2019; Cheng et al., 2016). These are mainly caused by the uncertainties in meteorological conditions (Sun et al., 2016) and emission inventories (Ma et al., 2018; Hong et al., 2017b; Sha et al.,

2019a), as well as unclear and/or inaccurate physical and chemical mechanisms associated with air pollutants (He and Zhang, 2014; He et al., 2015; Georgiou et al., 2018; Sha et al., 2019b). The inadequate inclusion or lack of cloud chemistry of SO_2 consumption simulations is one of the main causes (Ge et al., 2021; Cheng et al., 2016).. Therefore, it is very important and necessary to quantify the contribution of cloud chemistry in these typical regions in central-east China and get a better understand of multi-dimensional pollution interactions, especially between the upper layer and the surface.

This study is intended to use an on-line coupled chemical weather platform of WRF/CUACE, to analyze and evaluate the SO_2 in-cloud oxidation process in the four polluted regions in China, with two objectives: (1) evaluating the cloud chemistry scheme in WRF/CUACE by the in-situ cloud chemistry observations at Mount Tai in summers of 2015 and 2018; and (2) quantifying the contributions of cloud chemistry to the SO_2 and sulfate changes in a typical winter pollution month of December 2016 with a very long lasting heavy pollution episode. It is aimed to establish a system to assess the relative contribution of cloud chemistry to SO_2 oxidation and sulfate productions vs. other clear-sky processes.

2 Model description and Methodology

2.1 Cloud chemistry in WRF/CUACE

WRF/CUACE is an on-line coupled chemical weather model under the WRF frame work with a comprehensive chemical module - CUACE, which is developed at CMA (China Meteorological Administration) with a sectional aerosol physics, gas chemistry, aerosol-cloud interactions and thermodynamic equilibrium (Zhou et al., 2012; Zhou et al., 2016; Gong et al., 2003; Gong and Zhang, 2008; Zhang et al., 2021), with seven types of aerosols, i.e. black carbon, organic carbon, sulfate, nitrate, ammonium, soil dust, and sea salt, and more than 60 gaseous species. The aerosol size spectrum is divided into 12 bins with fixed boundaries of 0.005-0.01, 0.01-0.02, 0.02-0.04, 0.04-0.08, 0.08-0.16, 0.16-0.32, 0.32-0.64, 0.64-1.28, 1.28-2.56, 2.56-5.12, 5.12-10.24 and 10.24-20.48 μm. The system can simulate the concentrations of PM_{10}, $PM_{2.5}$ and O_3 as well as visibility. A complete heterogeneous chemistry module has been built in CUACE for nine gas-to-particle heterogeneous reactions including SO_2 to sulfate (Zhou et al., 2021; Zhang et al., 2021). The cloud chemistry mechanism in CUACE

considers the pathways of multiphase oxidation of SO_2 by H_2O_2 and O_3 in both stratocumulus and convective clouds (Gong et al., 2003; Von Salzen et al., 2000). The transport and chemical effects of sulfur in convective clouds are calculated based on a convective cloud model by WRF. Within the cloudy part of a grid box, the first-order rate constant (in s^{-1}) of S(IV) oxidation is given by the following expression:

$$F = \left| \frac{1}{C_{S(IV)}} \frac{dC_{S(IV)}}{dt} \right| = F_1 C_{O_3} + F_2 C_{H_2O_2} \qquad (1)$$

where $C_{S(IV)}$ is the total concentration of S(IV) (gas phase plus dissolved), C_{O_3} is the total concentration of O_3, and $C_{H_2O_2}$ is the total concentration of hydrogen peroxide.

The effective rate constants F_1 and F_2 are given by the following expressions:

$$F_1 = R_{O_3} f_1 \qquad (2)$$

$$F_2 = R_{H_2O_2} f_2 \qquad (3)$$

The reaction rate constants R_{O_3} and $R_{H_2O_2}$ refer to Maahs (1983) and Martin et al. (1984):

$$R_{O_3} = \left\{ 4.4 \times 10^{11} \exp(-4131/T) + 2.61 \times 10^3 \exp(-966/T) [H^+]^{-1} \right\} (Ms)^{-1} \qquad (4)$$

$$R_{H_2O_2} = 8 \times 10^4 \exp[-3650(1/T - 1/298)] \left\{ 0.1 + [H^+] \right\}^{-1} (Ms)^{-1} \qquad (5)$$

In Equations (2) and (3), the factors f_1 and f_2 represent the partitioning of the substance between the aqueous and gas phases and are determined by the Henry's law coefficients.

$$f_1 = \gamma f_{SO_2} f_{O_3} K_S \overline{K}_{HO} \qquad (6)$$

$$f_2 = \gamma f_{SO_2} f_{H_2O_2} \overline{K}_{HS} \overline{K}_{HP} \tag{7}$$

where γ is the dimensionless volume fraction of liquid water in the cloud. The parameters f_{SO_2}, f_{O_3} and $f_{H_2O_2}$ are the proportions of individual substances in the gas phase, which are calculated from the dimensionless Henry's law constant and γ.

$$f_{SO_2} = \left(1 + \gamma \overline{K}_{HS} K_S\right)^{-1} \tag{8}$$

$$f_{O_3} = \left(1 + \gamma \overline{K}_{HO}\right)^{-1} \tag{9}$$

$$f_{H_2O_2} = \left(1 + \gamma \overline{K}_{HP}\right)^{-1}$$
$$\tag{10}$$

with

$$K_S = \overline{K}_{HS}\left(1 + \frac{K_{1S}}{[H^+]} + \frac{K_{1S}K_{2S}}{[H^+]^2}\right) \tag{11}$$

The Henry's law constants used in (6) to (8) are listed in Table 1.

In order to consider the dependence of the oxidation rates on the pH, the H^+ concentration is calculated from ions balance.

$$[H^+] + [NH_4^+] = [OH^-] + 2[SO_4^{2-}] + 2[SO_3^{2-}] + [HSO_3^-] + [NO_3^-] + [HCO_3^-] \tag{12}$$

From Eqs. (1) ~ (12), CUACE can simulate the oxidation rates of SO_2 by H_2O_2 and O_3 mainly in the liquid and gaseous environment in both stratocumulus and convective clouds in three-dimensional way.

2.2 Assessment criteria

Three variables, RTCLD, DT, and RT, are defined to assess the impact of the cloud chemistry on SO$_2$ and sulfate. RTCLD refers to the concentration change ratio of substance i before and after the cloud chemical processes in a model run.

$$RTCLD(i) = 1 - \frac{BECLD(i)}{AFCLD(i)} \qquad (13)$$

where BECLD and AFCLD denote the concentrations of component i before and after the cloud chemical processes, respectively, and i denotes the chemical component of SO$_2$, O$_3$, H$_2$O$_2$, and sulfate.

The DT indicates the difference in concentration of substance i with (CLD) and without (nCLD) cloud chemistry module activated.

$$DT(i) = CLD(i) - nCLD(i) \qquad (14)$$

and the RT represents the concentration ratio change of the substance i with and without cloud chemistry in separate model runs:

$$RT(i) = 1 - \frac{nCLD(i)}{CLD(i)} \qquad (15)$$

2.3 Methodology

2.3.1 Model Evaluation – Case 1

Mount Tai with an altitude of 1483 meter, located in central Shandong Province, is the highest point of the North China Plain. It is an ideal observation site for cloud chemistry observation (Li et al., 2017; Li et al., 2020a; Li et al., 2020b). The observed concentrations of SO$_2$, O$_3$, H$_2$O$_2$ and sulfate in cloudy conditions from June 19 to July 30, 2015 and from June 20 to July 30, 2018 with time interval of 1 h are obtained to evaluate the cloud chemistry scheme in WRF/CUACE (Li et al., 2017; Li et al., 2020a; Li et

160 al., 2020b).

WRF/CUACE is set up with two-domain nesting for the evaluation, and the Riguan Peak is the central point (Fig. 1a). The horizontal resolution of outer domain (O) is 9 km with a grid of 100×104, and of the inner domain (I) is 3 km with a grid of 88×94 (Fig. 1a). There are 32 vertical layers with the top pressure of 100 hPa.

165 **2.3.2 Simulations of Regional Characteristics – Case 2**

The time period of December 2016 was selected to assess the regional contribution of cloud chemistry to SO_2 and sulfate in CUACE as a typical heavy pollution episode occurred from 16 to 21, covering most part of east China with the highest hourly $PM_{2.5}$ concentration exceeding 1100 μg m^{-3}. The simulation region is set up as shown in Figure 1b with two-level domain nesting. The outer domain 170 (O) covers Central and East Asia with a horizontal resolution of 54 km and a grid of 139×112. The inner domain (I) covers most of China on the eastern side of the Qinghai-Tibet Plateau including NCP, YRD, PRD and SCB, with a horizontal resolution of 18 km and a grid of 157×166. The vertical layer number of the model is the same as that in the Case 1.

Since the cloud water is the reaction pool of cloud chemistry, whether the simulation of cloud water 175 is reasonable or not is directly related to the effectiveness of cloud chemistry. Both the cloud water and rainwater from WRF are coupled to the cloud chemistry module and main physics configurations are listed in Table 2.

2.4 Meteorological, Pollution and Satellite Data

For both cases, the meteorological initial and boundary conditions for WRF/CUACE are from 180 National Centers for Environmental Prediction (NCEP) FNL global reanalysis at a resolution of 1°×1° with 6-h interval. The chemical lateral boundary conditions are from National Oceanic and Atmospheric Administration (NOAA) Meteorological Laboratory Regional Oxidant Model (NALROM) (Liu et al., 1996). The model is run in a restart way with a 5-day spin-up.

FY-2G cloud image data of CMA with an 1 h interval is used to evaluate the cloud in both cases. Routine observations in 3 h interval from 23 meteorological stations of CMA. Meteorological parameters include 2 m temperature, 2 m relative humidity, and 10 m wind speed. The hourly data from 55 city sites from the China National Environmental Monitoring Centre. are used to evaluate the meteorological fields and pollutants for December 2016. For one city, there are several observation sites, and these are averaged by excluding some obviously abnormal at one time and use the averaged data to presently the city.

The MEIC (Multi-resolution Emission Inventory for China) inventory, at a resolution of 0.25°, is used as the anthropogenic emissions with the species of sulfur dioxide (SO_2), nitrogen oxides (NO_x), carbon monoxide (CO), ammonia (NH_3), black carbon (BC), organic carbon (OC), non-methane volatile organic compounds (NMVOCs), $PM_{2.5}$ and PM_{10} from industry, transportation, residential, and agriculture (Li et al., 2017; Zheng et al., 2018). The emission base year of 2015 and 2017 are used for Case-1, of 2016 for Case-2, respectively.

3 Results and Discussions

3.1 Evaluation of the cloud chemistry mechanism

In order to verify the cloud chemistry mechanism in WRF/CUACE, the simulation results are compared with the observations at Mount Tai. By analyzing the satellite cloud images in and around Mount Tai and matching with the available observed data, two time periods with clouds from June 19 to July 30, 2015 and June 20 to July 30, 2018 are selected for the comparisons, defined as "cloud process-1" (CP-1) and "cloud process-2" (CP-2), respectively. The simulated results for chemical species are illustrated in scatter plots (Fig. 2), which reveals that the simulated concentrations of SO_2, sulfate, O_3, and H_2O_2 are all within a factor of two of the observations when cloud chemistry occurs, indicating reasonable agreement between simulations and observations for both CP-1 and CP-2 cases. The sulfate underestimates are clear in both CP-1 and CP-2 cases, which was reported by other modeling results before as well (Tuccella et al., 2012; Huang et al., 2019; Ge et al., 2022).

The statistics of correlation coefficients (R), relative average deviation (RAD), and normalized mean deviation (NMB) between hourly simulated and observed SO_2, O_3, H_2O_2 and sulfate are shown in Table 3. Among them, the simulated and observed averages of SO_2 are very close in both CP-1 and CP-2, with the RAD about -3.4% and -6.1% and with the RAD for other species in the range of 8.7-55.0%. The R for the four species are 0.34, 0.33 and 0.78 and 0.32 for CP-1, and 0.47, 0.40, 0.06 and 0.54 for CP-2, respectively. Although the R, RAD, and NMB of H_2O_2 in CP-2 is only 0.06, 18.0%, and -19.6%, the simulated mean value of H_2O_2 is closer to the observed mean value than that in CP-1 (RAD = 22.4%, NMB = -36.6%). For sulfate, the simulated Rs are 0.32 and 0.54 in CP-1 and CP-2, respectively, but the model underestimates sulfate concentrations with NMB of -71.0% and -59.4% in CP-1 and CP-2. Some reasons might contribute to the underestmations. First, the latitude of the observed site at Mount Tai is 1483 meters. So it can be in the boundary layer during the day time and in the free atmosphrere during the night time in summer (Zhu et al., 2022). Therefore, the diurnal variation of the boundary layer affects the three-dimensional concentration distribution of oxidants and aerosols (Zhao et al., 2013; Peng et al., 2021), and influences the development of cloud formation. Second, there have bias from the model due to the difficulties it represents the complex topography of Mount Tai and the cloud physics. Third, the cloud chemistry in CUACE lacks the pathway for TMI-catalyzed oxidation and NO_2-catalyzed oxidation as well as some other newly discovered oxidation mechanisms which can lead to the bias in SO_2 and sulfate. Forth, typical measurement systems for ambient aerosols easily misinterpret organosulfur (mainly in the presence of hydroxy-methane sulfonate (HMS)) as inorganic sulfate, thus leading to a positive observational bias, e.g., mean bias during winter haze in Beijing is 20% (Moch et al., 2018; Song et al., 2019).

Another interesting point that is simulated correctly by the model is the increasing trend of H_2O_2 and the decreasing trend of SO_2 from 2015 to 2018. The observed and simulated mean values of H_2O_2 are 26.5 and 16.8 μM in CP-1 in 2015, to 46.9 and 32.4 μM in CP-2 in 2018, respectively. For SO_2, the observed and simulated mean values are 2.2 and 2.3 μg/m³ in CP-1 in 2015, to 0.6 and 0.6 μg/m³ in CP-2 in 2018, respectively in Table 3. Both the observations and simulations show clearly the increasing trend of H_2O_2 and the decreasing trend of SO_2 from 2015 to 2018. This conclusion is consistent with the trends of other observational studies (Shen et al., 2012; Li et al., 2020b; Ren et al., 2009; Ye et al.,

2021). The SO_2 decreasing and H_2O_2 and O_3 increasing have been tightly attributed to the national SO_2 and particulate emission control measures since 2013 (Lu et al., 2020; Fan et al., 2021).

Figure 4 shows the RTCLD of SO_2 and simulated liquid water contents at 2:00 and 8:00 LST on both June 24 and June 25 in CP-1 at Mount Tai. The column cloud and the liquid water contents which are consistent with the cloud images indicate that there is cloud with sufficient water vapor in and around the vicinity of Mount Tai (Fig. 3). The SO_2 consumption rate (RTCLD(SO_2)) distribution is consistent with the liquid water distribution at all four times (Fig. 4). The SO_2 depletion rate is above 80% at Mount Tai which is compatible to the observation (Li et al., 2020). All of these indicate that the model can capture the SO_2 consumption in the cloudy environment.

In summary, SO_2, H_2O_2, O_3 and sulfate concentration are in the same order of the observations, and the mean values of SO_2 are close to the observed in the cloud chemistry comparison. WRF/CUACE is also able to simulate the decreasing trend of SO_2 and the increasing trends of O_3 and H_2O_2 with year. Therefore, the cloud chemistry mechanism in WRF/CUACE is relatively reasonable to reproduce the cloud chemistry for the gaseous pollutant SO_2, sulfate and the important oxidants of H_2O_2 and O_3.

3.2 Assessment of the impacts of cloud chemistry on regional SO_2 and sulfate

This session will further assess the contribution of cloud chemistry for the four main pollution regions of NCP, YRD, PRD, and SCB (Fig. 1) in China for the whole December of 2016 (as DEC thereafter) and a heavy pollution episode (as HPE thereafter) occurred during month (Dec. 16-22) as selected for Case 2.

3.2.1 Meteorological evaluation

As the driving force of air pollution and cloud chemistry, the simulated results of 2 m temperature (T2), 2 m relative humidity (RH2) and 10 m wind speed (WS10) in DEC and HPE are shows in Table 4. The temperature correlation is the best in DEC, followed by humidity and then wind speed, which is consistent with previous findings (Zhou et al., 2012; Wang et al., 2015; Gao et al., 2016). The RMSE of wind speeds all range from 1.03 to 1.50 m/s, falling within the criteria (less than 2 m/s) to define "good"

model performance in stagnant weather (Emery et al., 2001). The RSME of wind speed and the wind speed for HPE is smaller than that of DEC, which indicates that the model can relatively reasonably capture the static condition.

265   Figure 5 shows the satellite cloud images, the column cloud and the liquid water content simulated for the maturation and dissipation stages (19-22 Dec.) of the HPE. The satellite image shows that the cloud coverage region is mainly in the southwest of China besides SCB on the 19th, covering most of eastern China including NCP, YRD, PRD and SCB on the 20th and the 21st, and then moving eastward outside of China on the 22nd (Fig. 4 a1-d1). The cloud distribution fit well with the satellite images (Fig.

270   4 a2-d2) The column liquid water distribution also moves from west to east as the episode developed (Fig. 5 a3-d3), but is located more southern part of eastern China than that of the clouds. In SCB and YRD, the liquid water content is more abundant, reaching over 100.0 g/m^2, than that in PRD, only up to 10.0 g/m^2. NCP has the least liquid water content in the four regions, especially in Beijing, Tianjin and northwestern part of Hebei Province ranged 0.001~0.01 g/m^2, mostly due to the dry environment and

275   partly due to the overestimated temperature and underestimated humidity in Table 4. Above all, CUACE not only effectively simulates pollution but also provides a relatively reasonable meteorological background basis for cloud chemistry in the heavy pollution periods.

3.2.2 Chemical evaluation

The simulated hourly PM$_{2.5}$, O$_3$ and SO$_2$ concentrations in four regions are compared with the

280   observations (Table 5). The hourly PM$_{2.5}$, O$_3$ and SO$_2$ concentrations simulated in four regions are compared with the observations (Table 5). Most of the simulations are within a factor of two of the observations (figure omitted), and the mean values of the three pollutants in the four regions are close to the observations in DEC and HPE-2 in NCP, YRD, PRD and SCB. It is indicated that the model captures the variability of PM$_{2.5}$, O$_3$ and SO$_2$ concentrations for both DEC and HPE. During HPE-2, the

285   difference of mean values of SO$_2$ ranged from -7.6 to 10.4 µg/m^3, of O$_3$ ranged from -22 to 23.3 µg/m^3, and of PM$_{2.5}$ ranged from -156.5 to 48.8 µg/m^3. During DEC, the difference of mean values of SO$_2$ ranged from -21.5 to -1.2 µg/m^3, of O$_3$ ranged from 1.1 to 7.7 µg/m^3, and of PM$_{2.5}$ ranged from -71.3 to 1.3 µg/m^3. For PM$_{2.5}$, In the NCP, the R of HPE is 0.84, which is higher than the 0.39 of DEC in PRD.

In the NCP, the R of DEC is 0.62, which is higher than the 0.30 of HPE. The R is high for both DEC and HPE in YRD, with the value of 0.73 and 0.70. The differences of R between DEC and HPE are small in YRD and SCB. For SO_2, the model simulations are better for HPE in the three regions of NCP, YRD and SCB, than that for DEC. The Rs of HPE and DEC are 0.60 and 0.48 in NCP, 0.61 and 0.45 in YRD, and 0.49 and 0.19 in SCB, respectively. The correlations between observations and simulations for HPE and DEC in PRD are not significantly different, with R of 0.32 and 0.39, respectively.

The ability of CUACE to simulate SO_2, O_3 and sulfate concentrations have been validated in many previous research applications (Zhou et al., 2021; Zhang et al., 2021). Compared with the $PM_{2.5}$ concentrations simulated by WRF-CUACE used by Ke et al. (2020), the correlation is 0.41~0.85 in NCP, and 0.64~0.74 in YRD. The ability of other atmospheric models in China has the same performance such as NACRMS, and the correlation is about 0.68 for fine particulate matter in NCP during haze period (Wang et al., 2014).

The overall performance of the pollutants can be routinely observed from the surface network have been evaluated. Then, the following part of this paper will focus on assessing the effects of cloud chemical processes.

3.2.3 Assessment of regional contributions

The regional impacts of cloud chemical processes on surface SO_2 and sulfate are analyzed for DEC and for HPE. The pollution episode (HPE) is investigated with respect to the developing stage HPE-1 (Dec. 16-18, 2016), the maturity stage HPE-2 (Dec. 19-21, 2016) and to the dissipation stage HPE-3 (Dec. 22, 2016) for the four pollution regions of NCP, YRD, PRD and SCB.

Figure 6 is the mean sulfate concentration for DEC and HPE-2 for SO_2 and sulfate. The high and low centers of monthly mean SO_2 and sulfate concentrations of CUACE in December 2016 are coincided with the yearly average of the same year by Gao et al. (2021), in the SCB and NCP. For NCP, the mean sulfate concentration in Figure 6b is comparable to that by Wang et al. (2021) and Wang et al. (2022) in December 2016 as both of which increase from northwest to southeast almost in the same

magnitude. The sulfate concentrations are low on a monthly basis and high at the pollution maturity stage compared to the average of several pollution processes studied by Wang et al. (2022) in December 2016. The simulation of sulfate concentration is relatively reasonable in NCP. For SCB, sulfate concentrations are compatible to the observed in winter time in 2015 by Kong et al. (2020). The sulfate concentrations in Guangzhou is almost twice of the observations formed from aqueous-phase reactions in Zhou et al. (2020) and Guo et al. (2020).

The average impact of cloud chemistry on surface SO_2 and sulfate for DEC (Fig. 7, DT(SO_2) and DT (sulfate)) is assessed. It is found that SO_2 declination for DEC is concentrated mostly in the central-eastern part of China, by an average of 0.1-1.0 ppb in most regions by cloud chemistry. SO_2 concentrations are reduced by 0.5-3.0 ppb in most part of NCP, YRD, PRD and SCB regions. Among them, there is a relatively strong center by declining 3.0-10.0 ppb in SCB. Ge et al. (2021) have evaluated the effects of in-cloud aqueous-phase chemistry on SO_2 oxidation in the Community Earth System Model version 2 (CESM2). They found the results incorporating detailed cloud aqueous-phase chemistry greatly reduced SO_2 overestimation, which reduced by 0.1-10 ppb in China, and more than 10 ppb in some regions in Winter. This finding is consistent with the results demonstrated in Figure 7 of this study, where SO_2 concentrations are depleted by 0.1-10 ppb in China.

Correspondingly, sulfate growth is mainly centering in SCB, with the increased maximum center up to 20.0-50.0 $\mu g/m^3$. Sulfate concentrations are increased by 10.0-20.0 $\mu g/m^3$ in most part of NCP, YRD and PRD, and increased 5-10.0 $\mu g/m^3$ in others. The spatial distribution of cloud chemistry contribution to SO_2 and sulfate during HPE-2 is analyzed (Fig. 8, DT(SO_2) and DT(sulfate)) on the HPE-2. It is shown that the SO_2 concentration decreases most significantly in SCB, exceeding 1.0-3.0 ppb in most region, to 3.0-10.0 ppb in the central region. In YRD, PRD and NCP, the reduction reaches 1.0-3.0 ppb in most region while the smallest decrease is below 1.0 ppb in the northern part of NCP. Meanwhile, in terms of regional distribution, the regions of increasing sulfate and decreasing SO_2 concentrations are correlated, but not identical. Sulfate concentration increases by more than 10.0 $\mu g/m^3$ from the southern part of NCP to central China and from most of the eastern part of SCB to the YRD region. Sulfate concentration increases by more than 20.0 $\mu g/m^3$ in SCB and up to more than 50.0 $\mu g/m^3$ in the central

region of SCB, by 20.0-30.0 μg/m³ in the central region of YRD, and by 5.0-20.0 μg/m³ in the whole PRD region. The sulfate concentration increases up to 10.0 μg/m³ in the south of NCP and along the Yangtze River from the east of SCB to the west of YRD. In Figure 7b and figure 8b, the increasing rate for monthly mean sulfate concentrations is about 60% to 70% in NCP. Sulfate formation rates by H_2O_2 oxidation under winter haze conditions range from 10 to 1000 μg/m³/s, which is close to the range of 10 to 100 μg/m³/s tested by Wang et al. (2022) in several pollution episodes in December 2016. The heaviest and longest duration pollution episode that had a large number of clouds and high liquid water content (Fig. 5) on December 19-21, 2016, which are very favorable for the occurrence of in-cloud oxidation processes. Therefore, the in-cloud oxidation in this study is relatively reasonable.

In summary, comparing the contribution of cloud chemistry in DEC with HPE-2, it is found that the cloud chemistry in heavy pollution weather for SO_2 depletion and sulfate increase is mainly concentrated in the central-eastern part of China, and the four major pollution regions are also more obvious. However, SO_2 consumption and sulfate increase are not consistent, which is not only influenced by the local SO_2 concentration, but also by the cloud amount. Therefore, for SCB, where there is less polluted and has much more clouds than that in NCP, the impact of cloud chemistry on sulfate and its precursor SO_2 is always the most significant, for both HPE and DEC.

Exploring details into the HPE, three moments, 21:00 and 17:00 on the 20th and 21st of the HPE-2, and 12:00 on the 22nd of the HPE-3, are used to specifically analyze the contribution of cloud chemistry. It is found that the cloud chemistry influence is mainly on SCB and YRD at 21:00 LST on Dec. 20. The sulfate concentration increases (DT(sulfate)) by about 20.0-100.0 μg/m³ in most parts of SCB (Fig. 9a). The increase is about 10.0-40.0 μg/m³ in most parts of YRD. At 21st 17:00 LST, it is shown that the pollution episode has moved eastward and the cloud chemistry process has a stronger impact on NCP than at the previous time with about 10.0-60.0 μg/m³ in most regions (Fig. 9b). In PRD, the impact of the cloud chemistry is the least, with sulfate concentration increase of 10.0-40.0 μg/m³. At 22nd 12 LST. Although the episode has gradually dissipated, the impact still exist, with sulfate increase about 10.0-40.0 μg/m³ in most of these four regions (Fig. 9c).

Above all, the contribution of cloud chemistry to surface sulfate during this HPE is the highest in

the SCB, followed by the NCP, YRD and PRD, with mostly concentration increases range 20.0-100.0 $\mu g/m^3$, 10.0-60.0 $\mu g/m^3$, and 10.0-40.0 $\mu g/m^3$, 10.0-40.0 $\mu g/m^3$, respectively, and less 10.0 $\mu g/m^3$ in Beijing, Tianjin and the northwestern part of Hebei Province (Fig. 9). The observed $PM_{2.5}$ concentrations up to 350 $\mu g/m^3$ at 14:00 on the 20th and 236 $\mu g/m^3$ at 21:00 on the 20th in Chengdu in SCB, up to 80 $\mu g/m^3$ at 14:00 on the 20th and 77 $\mu g/m^3$ at 21:00 on the 20th in Hangzhou in YRD, were very high, partially supporting the cloud production of sulfate production at these specific times. At the same time, our model results showed that sulfate increases by cloud chemistry during these time periods were 10-20$\mu g/m^3$ and 20-30 $\mu g/m^3$ 14:00 and 21:00 on 20th at Chengdu, 30-60 $\mu g/m^3$ and 30-60 $\mu g/m^3$ at Hangzhou. Of particular note is the North China region, where the contribution of cloud chemistry is not significant on a monthly average but is very significant and exceeds that of the YRD region at certain moments during HPE. This also provides an explanation for the explosive increase in particulate matter concentrations during HPE in this region.

Further analysis of the simulation characteristics with and without cloud chemistry on all the regions during the HPE-2 stage (Fig. 10) and the DEC (Fig. 11), is carried out. Compared with nCLD, R of SO_2 in CLD increases by 0.60, 0.14, and 0.10 in YRD, SCB, and NCP, respectively, and the overestimation in NCP and PRD has been corrected during HPE-2. R also increases by 0.10, 0.03 and 0.04 in YRD, SCB and NCP for the DEC, respectively. It is obvious that the model simulates SO_2 concentrations better at NCP during HPE-2 than for DEC with cloud chemistry.

For $PM_{2.5}$, the statistical results of the simulated mean, R and NMB in CLD and nCLD in the four polluted regions do not differ significantly between HPE-2 and DEC, but there is a significant improvement in the underestimate in NCP and SCB. Under cloud chemistry, the deviation in the NCP increases from -45.7% to -35.7% for DEC and from -52.6% to -48.2% for HPE-2. The deviation in SCB increases from -44.2% to -29.1% for DEC and from -46.5% to -32.9% for HPE-2. A significant reduction in the model's $PM_{2.5}$ concentration simulation bias after considering cloud chemistry, and an improvement in the underestimation at NCP and SCB has been achieved.

Moreover, the statistical results of all stations (SUM in Fig. 12) show that after considering cloud chemical simulation (CLD), the NMB of SO_2 decreased from 39.3% to 13.8% and the NMB of sulfate

increased from -40.6% to -31.6% during the HPE-2 after the addition of cloud chemistry simulation, decreasing the simulation bias of both SO_2 and sulfate. This indicates that the addition of cloud chemistry to the model improves the model for SO_2 and sulfate simulations. The improvement of sulfate simulation in the presence of clouds also contributes to the improvement of the simulation accuracy of $PM_{2.5}$ mentioned above.

3.3 Site evaluation of cloud chemistry

"The statistical metrics of SO_2 and $PM_{2.5}$ hourly concentrations in 55 representative cities with and without cloud chemistry in the model were analyzed. The results indicate that most of the sites are improved with cloud chemistry in the SO_2 concentration simulation and 42 of the 55 cities are with the increasing R. In the $PM_{2.5}$ simulation, the correlations also are improved in some cities after the presence of cloud chemistry.

Representative sites of Beijing, Nanjing, Guangzhou and Chengdu at NCP, YRD, PRD and SCB are selected to quantify the impact of cloud chemistry during the HPE. The net depletion ratio of SO_2 column concentration ($RT(SO_2)$) during cloud chemistry is shown in Figure 13. It is found that SO_2 column concentration reduction maintained mostly a high value of over 60%, even to 80% sometimes, in Chengdu during HPE-2. In Nanjing, the SO_2 level is reduced by about 20-50% from 17th to 19th and up to 80% from 20th to 21st when the episode matures there. The changes of SO_2 in these two cities are consistent with the changes in cloud and liquid cloud water content distributions during the HPE-2 in Figure 3. The SO_2 reduction in Beijing and Guangzhou is consistently maintained at around 40% during the time from 17th to 21th. The lower oxidative transformation is related to the lower liquid water content in Beijing, while in Guangzhou it is attributed to the combination of low pollution levels and low cloud water content. Figure 3 shows that Chengdu maintained abundant water vapor conditions from 17th to 21st, and so does Nanjing from 20th to 21st. However, the ambient water vapor content is quite low in Guangzhou and Beijing throughout the process and the SO_2 oxidation is much lower than that of Chengdu and Nanjing. In conclusion, the cloud chemistry process can lead to SO_2 column concentration consumption share of more than 60% when cloud water content is abundant, which is also consistent with the observations of Mount Tai by Li (2020).

The impact of cloud chemistry (RT) on surface SO_2 and sulfate in four sites is also shown in Figure 13. The overall trend shows that the peak and valley regions of surface SO_2 consumption and sulfate increase are coincident. The cloud chemical processes of the surface SO_2 oxidation vary greatly between cities in different regions (Fig. 14a). In HPE-2, the percentage of surface SO_2 consumption can reach more than 90% in Chengdu and Nanjing, while it is below 30% in Beijing and Guangzhou, and does not reach 40% until the 22nd. Although the percentage of surface SO_2 consumption varies greatly, the increase in the percentage of sulfate does not vary so much between cities. In HPE-2, the increase in surface sulfate in the four cities ranges from 60-95% (Fig. 14b), and the sulfate increase rate interval contains the results summarized by Turnock et al. (2019).

Figure 15 is the variation of vertical profiles of sulfate increase by the cloud chemistry at the four times at 12:00 LST on 20 for HPE-2, at 04:00 LST on 21 for HPE-2, at 04:00 and 12:00 LST on 22 for HPE-3 in Beijing, Nanjing, Chengdu and Guangzhou. It shows that the sulfate produced by the cloud chemistry during this pollution process is concentrated mostly below 5 km in the troposphere, especially under 2 km. Again, less sulfate has been produced in Beijing in vertical than that of others by the cloud chemistry.

4. Summary and conclusions

The cloud chemistry mechanism in WRF/CUACE has been assessed by using the in-situ cloud chemistry observations of SO_2, O_3, and H_2O_2 from Mount Tai in June-July 2015 and 2018. The results show that the mechanism well captures the cloud processes for the oxidation of SO_2, reducing SO_2 by more than 80% during the cloudy phase, which is in good agreement with the observations.

The cloud chemistry contributions to the changes of SO_2 and sulfate concentrations in NCP, YRD, PRD and SCB regions are assessed by WRF/CUACE. During heavy pollution (HPE-2), the four regions are significantly affected by cloud chemistry, with SCB being the most obvious. The surface SO_2 reduction in SCB is up to 1.0-3.0 ppb and reaches 3.0-10.0 ppb in the high value areas, and surface sulfate concentration is increased by 10.0-30.0 $\mu g/m^3$ on average, with a maximum of more than 70.0 $\mu g/m^3$. Most areas in NCP, YRD and PRD have an average SO_2 reduction of 0.5-3.0 ppb and sulfate

increase of 5.0-30.0 μg/m^3. Meanwhile, the Beijing, Tianjin and the northwestern part of Hebei Province.of NCP has the least impact among the four typical cities of four regions. Although the monthly average impact of cloud chemistry is much weaker in the NCP due to less water vapor in December, the contribution of the southern part of NCP during heavy pollution time is still significant and cannot be ignored. In PRD, the contribution of cloud chemistry is weaker than other regions due to lighter pollution, although there are lots of clouds with abounded liquid water there. In addition, the cloud chemistry increases surface sulfate concentration by 60-95% and reduces surface SO_2 concentration by more than 80% in Beijing, Nanjing, Chengdu and Guangzhou in December during HPE-2, similar to that of previous studies (Turnock et al., 2019; Faloona et al., 2009). Above all, the average contribution of cloud chemistry during HPE-2 is significantly greater than that for DEC. Vertically, the cloud chemistry influence is mainly in the middle and lower troposphere below 2 km for four representative cities in HPE-2. Generally, the cloud chemistry can improve the model performance by reducing the overestimates of SO_2 and underestimates of sulfate.

This paper focuses on the cloud chemical mechanism evaluation, and assessed the contribution of cloud chemistry to SO_2 and sulfate changes. In the future, more mechanisms should be added to improve the cloud chemistry mechanism in CUACE to more accurately simulate SO_2 and sulfate and other aerosol components such as nitrate, ammonium, carbonate, and organic aerosols.

Code/data availability

All source code and data can be accessed by contacting the corresponding authors Sunling Gong (gongsl@cma.gov.cn).

Authors contribution

CZ and SG put forward the ideas and formulated overarching research goals. JL carried them out and wrote the manuscript with suggestions from all authors. LZ and JZ participated in the scientific interpretation and discussion. JC was assisted with data acquisition and processing. All authors contributed to the discussion and improvement of the manuscript.

Competing interests

The authors declare that they have no conflict of interest.

475 **Financial support**

This research has been supported by the National Key Project of the Ministry of Science and Technology of China (2022YFC3701205); CMA Innovation Development Project (CXFZ2021J023).

References

Alexander, B., Park, R. J., Jacob, D. J., and Gong, S.: Transition metal-catalyzed oxidation of atmospheric sulfur: Global implications for the sulfur budget, Journal of Geophysical Research: Atmospheres, 114, https://doi.org/10.1029/2008jd010486, 2009.

Buchard, V., da Silva, A. M., Colarco, P., Krotkov, N., Dickerson, R. R., Stehr, J. W., Mount, G., Spinei, E., Arkinson, H. L., and He, H.: Evaluation of GEOS-5 sulfur dioxide simulations during the Frostburg, MD 2010 field campaign, Atmos. Chem. Phys., 14, 1929-1941, https://doi.org/10.5194/acp-14-1929-2014, 2014.

Binkowski, F. S., and Roselle, S. J.: Models‐3 Community Multiscale Air Quality (CMAQ) model aerosol component 1. Model description, Journal of Geophysical Research: Atmospheres, 108, https://doi.org/10.1029/2001jd001409, 2003.

Caffrey, P., Hoppel, W., Frick, G., Pasternack, L., Fitzgerald, J., Hegg, D., Gao, S., Leaitch, R., Shantz, N., Albrechcinski, T., and Ambrusko, J.: In-cloud oxidation of SO_2 by O_3 and H_2O_2: Cloud chamber measurements and modeling of particle growth, Journal of Geophysical Research: Atmospheres, 106, 27587-27601, https://doi.org/10.1029/2000jd900844, 2001.

Chang, J. S., Brost, R. A., Isaksen, I. S. A., Madronich, S., Middleton, P., Stockwell, W. R., and Walcek, C. J.: A three-dimensional eulerian acid deposition model physical concepts and formulation, Journal of Geophysical Research: Atmospheres, 92, 14,681-614,700, https://doi.org/10.1029/jd092id12p14681, 1987.

Chapman, E. G., Gustafson, W. I., Easter, R. C., Barnard, J. C., and Fast, J. D.: Coupling aerosol-cloud-radiative processes in the WRF-Chem model: Investigating the radiative impact of elevated point sources, Atmos. Chem. Phys., 9, 945-964, https://doi.org/10.5194/acp-9-945-2009, 2009.

Chameides, W. L.: The photochemistry of a remote marine stratiform cloud, J. Geophys. Res., 89, 4739-4756, https://doi.org/10.1029/JD089iD03p04739, 1984.

Charlson, R. J., Schwartz, S. E., Hales, J. M., Cess, R. D., Coakley,. A., JR., Hansen, J. E., and Hofmann, D. J.: Climate forcing by anthropogenic aerosols, Science, 255, 423-423, https://doi.org/10.1126/science.255.5043.423, 1992.

Emery, C., Tai, E., and Yarwood, G.: Enhanced meteorological modeling and performance evaluation for two Texas ozone episodes, Biology, Corpus ID: 127579774, 2001.

Cheng, Y., Zheng, G., Wei, C., Mu, Q., Zheng, B., Wang, Z., Gao, M., Zhang, Q., He, K., and Carmichael, G.: Reactive nitrogen chemistry in aerosol water as asource of sulfate during haze events in China, Science Advances, https://doi.org/10.1126/sciadv.1601530, 2016.

Dovrou, E., Rivera-Rios, J. C., Bates, K. H., and Keutsch, F. N.: Sulfate Formation via Cloud Processing from Isoprene Hydroxyl Hydroperoxides (ISOPOOH), Environ Sci Technol, 53, 12476-12484, https://doi.org/10.1021/acs.est.9b04645, 2019.

Ervens, B.: Modeling the Processing of Aerosol and Trace Gases in Clouds and Fogs, Chemical Reviews, 115, 4157-4198, https://doi.org/10.1021/cr5005887, 2015.

Faloona, I.: Sulfur processing in the marine atmospheric boundary layer: A review and critical assessment of modeling uncertainties, Atmospheric Environment, 43(18), 2841-2854, https://doi.org/10.1016/j.atmosenv.2009.02.043, 2009.

Faloona, I., Conley, S. A., Blomquist, B., Clarke, A. D., Kapustin, V., Howell, S., Lenschow, D. H., and Bandy, A. R.: Sulfur dioxide in the tropical marine boundary layer: dry deposition and heterogeneous oxidation observed during the Pacific Atmospheric Sulfur Experiment, Journal of Atmospheric Chemistry, 63,

Fan, D., Ye. Y., and Wang, W.: Air Pollution Control and Public Health:Evidence from "Air Pollution Prevention and Control Action Plan" in China, Statistical Research, 38(9), 60-74, https://doi.org/10.19343/j.cnki.11-1302/c.2021.09.005, 2021. 13-32, https://doi.org/10.1007/s10874-010-9155-0, 2010.

Gao, M., Carmichael, G. R., Wang, Y., Ji, D., Liu, Z., and Wang, Z.: Improving simulations of sulfate aerosols during winter haze over Northern China: the impacts of heterogeneous oxidation by NO_2, Frontiers of Environmental Science & Engineering, 10, 11, https://doi.org/10.1007/s11783-016-0878-2, 2016.

Ge, W., Liu, J., Xiang, S., Zhou, Y., Zhou, J., Hu, X., Ma, J., Wang, X., Wan, Y., Hu, J., Zhang, Z., Wang, X., Tao, S.: Improvement and Uncertainties of Global Simulation of Sulfate Concentration and Radiative Forcing in CESM2, https://doi.org/10.1002/essoar.10512154.1, 2022.

Ge, W., Liu, J., Yi, K., Xu, J., Zhang, Y., Hu, X., Ma, J., Wang, X., Wan, Y., Hu, J., Zhang, Z., Wang, X., and Tao, S.: Influence of atmospheric in-cloud aqueous-phase chemistry on global simulation of SO_2 in CESM2, Atmos. Chem. Phys., https://doi.org/10.5194/acp-2021-406, 2021.

Georgiou, G. K., Christoudias, T., Proestos, Y., Kushta, J., Hadjinicolaou, P., and Lelieveld, J.: Air quality modelling in the summer over the eastern Mediterranean using WRF-Chem: chemistry and aerosol mechanism intercomparison, Atmos. Chem. Phys., 18, 1555-1571, https://doi.org/10.5194/acp-18-1555-2018, 2018.

Gen, M., Zhang, R., Huang, D. D., Li, Y., Chan, C. K.: Heterogeneous SO_2 Oxidation in Sulfate Formation by Photolysis of Particulate Nitrate, Environ. Sci. Technol, 6 (2), 86−91, https://doi.org/10.1021/acs.estlett.8b00681, 2019a.

Gen, M., Zhang, R., Huang, D. D., Li, Y., and Chan, C. K.: Heterogeneous Oxidation of SO(2) in Sulfate Production during Nitrate Photolysis at 300 nm: Effect of pH, Relative Humidity, Irradiation Intensity, and the Presence of Organic Compounds, Environ Sci Technol, 53, 8757-8766, https://doi.org/10.1021/acs.est.9b01623, 2019b.

Gong, S., and Zhang, X.: CUACE/Dust – an integrated system of observation and modeling systems for operational dust forecasting in Asia, Atmospheric Chemistry and Physics, 8, 2333-2340,

https://doi.org/10.5194/acp-8-2333-2008, 2008.

Gong, S. L., Barrie, L. A., Blanchet, J.-P., von Salzen, K., Lohmann, U., Lesins, G., Spacek, L., Zhang, L. M., Girard, E., Lin, H., Leaitch, R., Leighton, H., Chylek, P., and Huang, P.: Canadian Aerosol Module: A size-segregated simulation of atmospheric aerosol processes for climate and air quality models 1. Module development, Journal of Geophysical Research: Atmospheres, 108, https://doi.org/10.1029/2001jd002002, 2003.

Guo, J., Wang, Y., Shen, X., Wang, Z., Lee, T., Wang, X., Li, P., Sun, M., Jeffrey, L., Collett, J., Wang, W., and Wang, T.: Characterization of cloud water chemistry at Mount Tai, China: Seasonal variation, anthropogenic impact, and cloud processing, Atmospheric Environment, 60, 467-476, https://doi.org/10.1016/j.atmosenv.2012.07.016, 2012.

Guo, S., Hu, M., Zamora, M. L., Peng, J., Shang, D., Zheng, J., Du, Z., Wu, Z., Shao, M., Zeng, L., Molina, M. J., and Zhang, R.: Elucidating severe urban haze formation in China, Proceedings of the National Academy of Sciences, 111, 17373-17378, https://doi.org/10.1073/pnas.1419604111, 2014.

Harris, E., Sinha, B., van Pinxteren, D., Tilgner, A., Fomba, K. W., Schneider, J., Roth, A., Gnauk, T., Fahlbusch, B., Mertes, S., Lee, T., Collett, J., Foley, S., Borrmann, S., Hoppe, P., and Herrmann, H.: Enhanced role of transition metal ion catalysis during in-cloud oxidation of SO_2, Science, 340, 727-730, https://doi.org/10.1126/science.1230911, 2013.

He, J. and Zhang, Y.: Improvement and further development in CESM/CAM5: gas-phase chemistry and inorganic aerosol treatments, Atmos. Chem. Phys., 14, 917-9200, https://doi.org/10.5194/acp-14-9171-2014, 2014.

He, J., Zhang, Y., Glotfelty, T., He, R., Bennartz, R., Rausch, J., and Sartelet, K.: Decadal simulation and comprehensive evaluation of CESM/CAM5.1 with advanced chemistry, aerosol microphysics, and aerosol-cloud interactions, Journal of Advances in Modeling Earth Systems, 7, 110-141, https://doi.org/10.1002/2014ms000360, 2015.

575   Hong, C., Zhang, Q., Zhang, Y., Tang, Y., Tong, D., and He, K.: Multi-year downscaling application of two-way coupled WRF v3.4 and CMAQ v5.0.2 over east Asia for regional climate and air quality modeling: model evaluation and aerosol direct effects, Geosci. Model Dev., 10, 2447-2470, https://doi.org/10.5194/gmd-10-2447-2017, 2017a.

Hong, C., Zhang, Q., He, K., Guan, D., Li, M., Liu, F., and Zheng, B.: Variations of China's emission
580   estimates: response to uncertainties in energy statistics, Atmos. Chem. Phys., 17, 1227-1239, https://doi.org/10.5194/acp-17-1227-2017, 2017b.

Huang, L., An, J., Koo, B., Yarwood, G., Yan, R., Wang, Y., Huang, C., and Li, L.: Sulfate formation during heavy winter haze events and the potential contribution from heterogeneous $SO_2 + NO_2$ reactions in the Yangtze River Delta region, China, Atmos. Chem. Phys., 19, 14311–14328,
585   https://doi.org/10.5194/acp-19-14311-2019, 2019.

Hung, H. M., Hsu, M. N., and Hoffmann, M. R.: Quantification of SO_2 Oxidation on Interfacial Surfaces of Acidic Micro-Droplets: Implication for Ambient Sulfate Formation, Environ Sci Technol, 52, 9079-9086, https://doi.org/10.1021/acs.est.8b01391, 2018.

Ke, H., Gong, S., He, J., Zhou, C., Zhang, L., Zhou, Y.: Assessment of Open Biomass Burning Impacts
590   on Surface $PM_{2.5}$ Concentration, Chinese Academy of Meteorological Sciences, 31, 105-106, https://doi.org/10.11898/1001-7313.20200110, 2020.

Kong, L., Tan, Q., Feng, M., Qu, Y., An, J., Liu, X., Cheng, N., Deng, Y., Zhai, R., and Wang, Z.: Investigating the characteristics and source analyses of $PM_{2.5}$ seasonal variations in Chengdu, Southwest China, Chemosphere, 243, 125267, https://doi.org/10.1016/j.chemosphere.2019.125267, 2020.

595   Kotarba, A. Z.: Calibration of global MODIS cloud amount using CALIOP cloud profiles, Atmospheric Measurement Techniques, 13, 4995-5012, https://doi.org/10.5194/amt-13-4995-2020, 2020.

IIbusuki, T., and Takeuchi, K.: Sulfur dioxide oxidation by oxygen catalyzed by mixtures of manganese(II) and iron(III) in aqueous solutions at environmental reaction conditions, Atmospheric

Environment, 21, 1555-1560, https://doi.org/10.1016/0004-6981(87)90317-9, 1987.

600   Ivanova, I. T., and Leighton, H. G.: Aerosol-Cloud Interactions in a Mesoscale Model. Part II: Sensitivity to Aqueous-Phase Chemistry, Journal of the Atmospheric Sciences, 65, 309-330, https://doi.org/10.1175/2007JAS2276.1, 2008.

Leighton, H. G., and Ivanova, I. T.: Aerosol–Cloud Interactions in a Mesoscale Model. Part I: Sensitivity to Activation and Collision–Coalescence, Journal of the Atmospheric Sciences, 65, 289-308,
605   https://doi.org/10.1175/2007jas2207.1, 2008.

Lelieveld, J., and Heintzenberg, J.: Sulfate cooling effect on climate through in-cloud oxidation of anthropogenic SO_2, Science, 285, 117-120, https://doi.org/10.1126/science.258.5079.117, 1992.

Leighton, H. G., Yau M. K., Macdonald, A. M., Pitre, J. S., and Giles, A.: A numerical simulation of the chemistry of a rainband, Atmospheric Environment, 24, 1211-1217, https://doi.org/10.1016/0960-
610   1686(90)90086-3, 1990.

Li, J. R.: Microphysical Characteristics and S(IV) Multiphase Chemical Reaction Mechanism of Orographic Clouds, Ph.D. thesis, Fudan University, 127pp, 2020.

Li, J., Wang, X., Chen, J., Zhu, C., Li, W., Li, C., Liu, L., Xu, C., Wen, L., Xue, L., Wang, W., Ding, A., and Herrmann, H.: Chemical composition and droplet size distribution of cloud at the summit of Mount
615   Tai, China, Atmos. Chem. Phys., 17, 9885-9896, https://doi.org/10.5194/acp-17-9885-2017, 2017.

Li, J., Zhu, C., Chen, H., Fu, H., Xiao, H., Wang, X., Herrmann, H., and Chen, J.: A More Important Role for the Ozone‐S(IV) Oxidation Pathway Due to Decreasing Acidity in Clouds, Journal of Geophysical Research: Atmospheres, 125, https://doi.org/10.1029/2020jd033220, 2020a.

Li, J., Zhu, C., Chen, H., Zhao, D., Xue, L., Wang, X., Li, H., Liu, P., Liu, J., Zhang, C., Mu, Y., Zhang,
620   W., Zhang, L., Herrmann, H., Li, K., Liu, M., and Chen, J.: The evolution of cloud and aerosol microphysics at the summit of Mt. Tai, China, Atmos. Chem. Phys., 20, 13735-13751,

https://doi.org/10.5194/acp-20-13735-2020, 2020b.

Li, M., Liu, H., Geng, G., Hong, C., Liu, F., Song, Y., Tong, D., Zheng, B., Cui, H., Man, H., Zhang, Q., and He, K.: Anthropogenic emission inventories in China: a review, Natl. Sci. Rev., 4, 834-866, https://doi.org/10.1093/nsr/nwx150, 2017.

Li, P. F.: Fog Water Chemistry and Fog-Haze Transformation in Shanghai, Fudan University, Ph.D. thesis, 145pp.

Liu, S. C., McKeen, S. A., Hsie, E.-Y., Lin, X., Kelly, K. K., Bradshaw, J. D., Sandholm, S. T., Browell, E. V., Gregory, G. L., Sachse, G. W., Bandy, A. R., Thornton, D. C., Blake, D. R., Rowland, F. S., Newell, R., Heikes, B. G., Singh, H., and R. W. Talbot: Model study of tropospheric trace species distributions during PEM-WEST A, Journal of Geophysical Research: Atmospheres, 101, https://doi.org/0148-0227/96/95JD-02277505.00, 1996.

Liu, T., Chan, A. W. H., and Abbatt, J. P. D.: Multiphase Oxidation of Sulfur Dioxide in Aerosol Particles: Implications for Sulfate Formation in Polluted Environments, Environ Sci Technol, 55, 4227-4242, https://doi.org/10.1021/acs.est.0c06496, 2021.

Lu, X., Zhang, S., Xing, J., Wang, Y., Chen, W., Ding, D., Wu, Y., Wang, S., Duan, L., and Hao, J.: Progress of Air Pollution Control in China and Its Challenges and Opportunities in the Ecological Civilization Era, Engineering., 6 (12), 1423-1431, https://doi.org/10.1016/j.eng.2020.03.014, 2020.

Maahs, H. G.: Kinetics and Mechanism of the Oxidation of S(IV) by Ozone in Aqueous Solution With Particular Reference to SO_2 Conversion in Nonurban Tropospheric Clouds, journal of geophysical research oceans, 88, 10721-10732, https://doi.org/10.1029/JC088iC15p10721, 1983.

Martin, G. M., Johnson D. W., and Spice A., The measurement and parameterization of effective radius in warm stratocumulus cloud, J. Atmos. Sci., 51, 1823-1842, https://doi.org/10.1175/1520-0469(1994)051<1823:TMAPOE>2.0.CO;2, 1994.

645   Martin, L. R., and Good, T. W.: Catalyzed oxidation of sulfur dioxide in solution: The iron-manganese synergism, Atmospheric Environment, 25, 2395-2399, https://doi.org/10.1016/0960-1686(91)90113-L, 1991.

Menut, L., Bessagnet, B., Khvorostyanov, D., Beekmann, M., Colette, A., Coll, I., Curci, G., Foret, G., Hodzic, A., Mailler, S., Meleux, F., Monge, J. L., Pison, I., Turquety, S., Valari, M., Vautard, R., and

650   Vivanco, M. G.: Regional atmospheric composition modeling with CHIMERE, Geoscientific Model Development, 6, 981-1028, https://doi.org/10.5194/gmdd-6-203-2013, 2013.

Molina, L. T, and Molina, M. J..: Air Quality in the Mexico Megacity: An Integrated Assessment, Alliance for Global Sustainability Bookseries, https://doi.org/10.1007/978-94-010-0454-1, 2002.

Park, R. J., and Jacob, D. J.: Sources of carbonaceous aerosols over the United States and implications

655   for natural visibility, Journal of Geophysical Research, 108, https://doi.org/10.1029/2002jd003190, 2003.

Peng, J., Hu, M., Shang, D. J., Wu, Z., Du, Z., Tan, T., Wang, Y., Zhang, F., and Zhang, R.: Explosive secondary aerosol formation during severe haze in the North China Plain, Environ Sci Technol 55(4), 2189-2207, https://doi.org/10.1021/acs.est.0c07204, 2021.

660   Pye, H. O. T., Nenes, A., Alexander, B., Ault, A. P., Barth, M. C., Clegg, S. L., Jr., J. L. C., Fahey, K. M., Hennigan, C. J., Herrmann, H., Kanakidou, M., Kelly, J. T., Ku, I.-T., McNeill, V. F., Riemer, N., Schaefer, T., Shi, G., Tilgner, A., Walker, J. T., Wang, T., Weber, R., Xing, J., Zaveri, R. A., and Zuend, a. A.: Havala O. T. Pye The acidity of atmospheric particles and clouds, Atmos. Chem. Phys., 20, 4809-4888, https://doi.org/10.5194/acp-20-4809-2020, 2020.

665   Ramanathan, V., Crutzen, P. J., Kiehl, J. T., and Rosenfeld, D.: Aerosols, climate, and the hydrological cycle, Science, 294, 2119-2124, https://doi.org/10.1126/science.1064034, 2001.

Ravishankara, A. R.: Heterogeneous and Multiphase Chemistry in the Troposphere, Science, 276, 1058-1065, https://doi.org/10.1126/science.276.5315.1058, 1997.

Ren, Y., Ding, A., Wang, T., Shen, X., Guo, J., Zhang, J., Wang, Y., Xu, P., Wang, X., and Gao, J.: Measurement of gas-phase total peroxides at the summit of Mount Tai in China, Atmospheric Environment, 43, 1702-1711, https://doi.org/10.1016/j.atmosenv.2008.12.020, 2009.

Sun, K., Liu, H., Ding, A., and Wang, X.: WRF-Chem Simulation of a Severe Haze Episode in the Yangtze River Delta, China, Aerosol Air Qual. Res., 16, 1268-1283, https://doi.org/10.4209/aaqr.2015.04.0248, 2016.

Sha, T., Ma, X. Y., Jia, H. L., van der A, R. J., Ding, J. Y., Zhang, Y. L., and Chang, Y. H.: Exploring the influence of two inventories on simulated air pollutants during winter over the Yangtze River Delta, Atmos. Environ., 206, 170-182, https://doi.org/10.1016/j.atmosenv.2019.03.006, 2019a.

Sha, T., Ma, X., Jia, H., Tian, R., Chang, Y., Cao, F., and Zhang, Y.: Aerosol chemical component: Simulations with WRF-Chem and comparison with observations in Nanjing, Atmospheric Environment, 218, https://doi.org/10.1016/j.atmosenv.2019.116982, 2019b.

Shen, X., Lee, T., Guo, J., Wang, X., Li, P., Xu, P., Wang, Y., Ren, Y., Wang, W., Wang, T., Li, Y., Carn, S. A., and Collett, J. L.: Aqueous phase sulfate production in clouds in eastern China, Atmospheric Environment, 62, 502-511, https://doi.org/10.1016/j.atmosenv.2012.07.079, 2012.

Shimadera, H., Kondo, A., Shrestha, K. L., Kaga, A., and Inoue, Y.: Annual sulfur deposition through fog, wet and dry deposition in the Kinki Region of Japan - ScienceDirect, Atmospheric Environment, 45, 6299-6308, https://doi.org/10.1016/j.atmosenv.2011.08.055, 2011.

Sielski, J., Kazirod-Wolski, K., Jozwiak, M. A., and Jozwiak, M.: The influence of air pollution by PM2.5, PM10 and associated heavy metals on the parameters of out-of-hospital cardiac arrest, Sci Total Environ, 788, 147541, https://doi.org/10.1016/j.scitotenv.2021.147541, 2021.

Song, S., Nenes, A., Gao, M., Zhang, Y., Liu, P., Shao, J., Ye, D., Xu, W., Lei, L., Sun, Y., Liu, B., Wang, S., and McElroy, M. B.: Thermodynamic Modeling Suggests Declines in Water Uptake and Acidity of Inorganic Aerosols in Beijing Winter Haze Events during 2014/2015–2018/2019, Environmental Science

& Technology Letters, 6, 752-760, htttps://doi.org/10.1021/acs.estlett.9b00621, 2019.

Terrenoire, E., Bessagnet, B., Rouïl, L., Tognet, F., Pirovano, G., Létinois, L., Beauchamp, M., Colette, A., Thunis, P., Amann, M., and Menut, L.: High-resolution air quality simulation over Europe with the chemistry transport model CHIMERE, Geoscientific Model Development, 8, 21-42, https://doi.org/10.5194/gmd-8-21-2015, 2015.

Tie, X.: Assessment of the global impact of aerosols on tropospheric oxidants, Journal of Geophysical Research, 110, https://doi.org/10.1029/2004jd005359, 2005.

Tremblay, A., and Leighton, H.: A Three-Dimensional Cloud Chemistry Model, Journal of Climate & Applied Meteorology, 25, 652-671, https://doi.org/10.1016/1352-2310(96)00063-5, 1986.

Tuccella, P., Curci, G., Visconti, G., Bessagnet, B., Menut, L., Park, R.: Modeling of gas and aerosol with WRF/Chem over Europe: Evaluation and sensitivity study, Journal of Geophysical Research, 117, https://doi.org/10.1029/2011JD016302, 2012.

Turnock, S. T., Mann, G. W., Woodhouse, M. T., Dalvi, M., O'Connor, F. M., Carslaw, K. S., and Sprackle, D. V.: The Impact of Changes in Cloud Water pH on Aerosol Radiative Forcing, Geophysical Research Letters, 46, 4039 – 4048, https://doi.org/10.1029/2019GL082067, 2019.

Twomey S.: Aerosols, clouds and radiation, Atmospheric Environment. part A. general Topics, 25, 2435-2442, https://doi.org/10.1016/0960-1686(91)90159-5, 1991.

Twomey, S. A., Piepgrass, M., and Wolfe, T. L.: An assessment of the impact of pollution on the global cloud albedo, Tellus B: Chemical and Physical Meteorology, 36B, 356-366, https://doi.org/10.1111/j.1600-0889.1984.tb00254.x, 1984.

von Salzen, K., Leighton, H. G., Ariya, P. A., Barrie, L. A., Gong, S. L., Blanchet, J. P., Spacek, L., Lohmann, U., and Kleinman, L. I.: Sensitivity of sulphate aerosol size distributions and CCN concentrations over North America to SOx emissions and H_2O_2 concentrations, Journal of Geophysical

Research: Atmospheres, 105, 9741-9765, https://doi.org/10.1029/2000jd900027, 2000.

Wang, G., Zhang, R., Gomez, M. E., Yang, L., Levy Zamora, M., Hu, M., Lin, Y., Peng, J., Guo, S., Meng, J., Li, J., Cheng, C., Hu, T., Ren, Y., Wang, Y., Gao, J., Cao, J., An, Z., Zhou, W., Li, G., Wang, J., Tian, P., Marrero-Ortiz, W., Secrest, J., Du, Z., Zheng, J., Shang, D., Zeng, L., Shao, M., Wang, W., Huang, Y., Wang, Y., Zhu, Y., Li, Y., Hu, J., Pan, B., Cai, L., Cheng, Y., Ji, Y., Zhang, F., Rosenfeld, D., Liss, P. S., Duce, R. A., Kolb, C. E., and Molina, M. J.: Persistent sulfate formation from London Fog to Chinese haze, Proc Natl Acad Sci U S A, 113, 13630-13635, https://doi.org/10.1073/pnas.1616540113, 2016.

Wang, H., Shi, G. Y., Zhang, X. Y., Gong, S. L., Tan, S. C., Chen, B., Che, H. Z., and Li, T.: Mesoscale modelling study of the interactions between aerosols and PBL meteorology during a haze episode in China Jing-Jin-Ji and its near surrounding region - Part 2: Aerosols' radiative feedback effects, Atmos. Chem. Phys., 15, 6(2015-03-23), 14, 3277-3287, https://doi.org/10.5194/acp-15-3257-2015, 2015.

Wang, J., Li, J., Ye, J., Zhao, J., Wu, Y., Hu, J., Liu, D., Nie, D., Shen, F., Huang, X., Huang, D. D., Ji, D., Sun, X., Xu, W., Guo, J., Song, S., Qin, Y., Liu, P., Turner, J. R., Lee, H. C., Hwang, S., Liao, H., Martin, S. T., Zhang, Q., Chen, M., Sun, Y., Ge, X., and Jacob, D. J.: Fast sulfate formation from oxidation of SO_2 by NO_2 and HONO observed in Beijing haze, Nature Communications, 11, https://doi.org/10.1038/s41467-020-16683-x, 2020.

Wang, S., Zhou, S., Tao, Y., Tsui, W. G., Ye, J., Yu, J. Z., Murphy, J. G., McNeill, V. F., Abbatt, J. P. D., and Chan, A. W. H.: Organic Peroxides and Sulfur Dioxide in Aerosol: Source of Particulate Sulfate, Environ Sci Technol, 53, 10695-10704, https://doi.org/10.1021/acs.est.9b02591, 2019.

Wang, T., Liu, M., Liu, M., Song, Y., Xu, Z., Shang, F., Huang, X., Liao, W., Wang, W., Ge, M., Cao, J., Hu, J., Tang, G., Pan, Y., Hu, M., and Zhu, T.: Sulfate Formation Apportionment during Winter Haze Events in North China, Environ. Sci. Technol., 56(12), 7771-7778, https://doi.org/10.1021/acs.est.2c02533, 2022.

Wang, W., Liu, M., Wang, T., Song, Y., Zhou, L., Cao, J., Hu, J., Tang, G., Chen, Z., Li, Z., Xu, Z., Peng,

C., Lian, C., Chen, Y., Pan, Y., Zhang, Y., Sun, Y., Li, W., Zhu, T., Tian, H., and Ge, M.: Sulfate formation is dominated by manganese-catalyzed oxidation of SO_2 on aerosol surfaces during haze events, Nature Communications, 12(1), https://doi.org/10.1038/s41467-021-22091-6, 2021.

Wang, Z., Wang, Z., Li, J., Zheng H., Yan P., Li, J.: Development of a Meteorology-Chemistry Two-Way Coupled Numerical Model (WRF-NAQPMS) and Its Application in a Severe Autumn Haze Simulation over the Beijing-Tianjin-Hebei Area, China, Climatic and Environmental Research, 19(2), 153-163, https://doi.org/10.3878/j.issn.1006-9585.2014.13231, 2014.

Wei, Y., Chen, X., Chen, H., Li, J., Wang, Z., Yang, W., Ge, B., Du, H., Hao, J., Wang, W., Li, J., Sun, Y., and Huang, H.: IAP-AACM v1.0: a global to regional evaluation of the atmospheric chemistry model in CAS-ESM, Atmos. Chem. Phys., 19, 8269-8296, https://doi.org/10.5194/acp-19-8269-2019, 2019.

Xie, Y., Dai, H., Zhang, Y., Wu, Y., Hanaoka, T., and Masui, T.: Comparison of health and economic impacts of $PM_{2.5}$ and ozone pollution in China, Environ Int, 130, 104881, https://doi.org/10.1016/j.envint.2019.05.075, 2019.

Yao, S., Wang, Q., Zhang, J., and Zhang, R.: Characteristics of Aerosol and Effect of Aerosol-Radiation-Feedback in Handan, an Industrialized and Polluted City in China in Haze Episodes, Atmosphere, 12, 670, https://doi.org/10.3390/atmos12060670, 2021.

Yao, M., Zhao, Y., Hu, M., Huang, D., Wang, Y., Yu, J. Z., and Yan, N.: Multiphase Reactions between Secondary Organic Aerosol and Sulfur Dioxide: Kinetics and Contributions to Sulfate Formation and Aerosol Aging, Environmental Science & Technology Letters, 6, 768-774, htttps://doi.org/10.1021/acs.estlett.9b00657, 2019.

Ye, C., Xue, C., Zhang, C., Ma, Z., Liu, P., Zhang, Y., Liu, C., Zhao, X., Zhang, W., He, X., Song, Y., Liu, J., Wang, W., Sui, B., Cui, R., Yang, X., Mei, R., Chen, J., and Mu, Y.: Atmospheric Hydrogen Peroxide H_2O_2 at the Foot and Summit of Mt Tai Variations Sources, Journal of Geophysical Research: Atmospheres, 126, https://doi.org/10.1029/2020JD033975, 2021.

765 Ye, J., Abbatt, J. P. D., and Chan, A. W. H.: Novel pathway of SO_2 oxidation in the atmosphere: reactions with monoterpene ozonolysis intermediates and secondary organic aerosol, Atmos. Chem. Phys., 18, 5549-5565, htttps://doi.org/10.5194/acp-18-5549-2018, 2018.

Yuan, D. M., and Ma, X. H.: The severe haze process in 16－21 December 2016 and associated atmospheric circulation anomalies [J]. Climatic and Environmental Research (in Chinese), 22 (6): 757-
770 764, https://doi.org/10.3878/j.issn.1006-9585.2017.17029, 2017.

Zhang, L., Gong, S., Zhao, T. L., Zhou, C. H., and Zhang, X. Y.: Development of WRF/CUACE v1.0 model and its preliminary application in simulating air quality in China, Geoscientific Model Development, https://doi.org/10.5194/gmd-14-703-2021, 2021.

Zhang, X. Y., Wang, Y. Q., Niu, T., Zhang, X. C., Gong, S. L., Zhang, Y. M., and Sun, J. Y.: Atmospheric
775 aerosol compositions in China: spatial/temporal variability, chemical signature, regional haze distribution and comparisons with global aerosols, Atmos. Chem. Phys., 12, 779-799, https://doi.org/10.5194/acp-12-779-2012, 2012.

Zheng, B., Tong, D., Li, M., Liu, F., Hong, C., Geng, G., Li, H., Li, X., Peng, L., Qi, J., Yan, L., Zhang, Y., Zhao, H., Zheng, Y., He, K., and Zhang, Q.: Trends in China's anthropogenic emissions since 2010 as
780 the consequence of clean air actions, Atmos. Chem. Phys., 18, 14095-14111, https://doi.org/10.5194/acp-18-14095-2018, 2018.

Zheng, B., Zhang, Q., Zhang, Y., He, K. B., Wang, K., Zheng, G. J., Duan, F. K., Ma, Y. L., and Kimoto, T.: Heterogeneous chemistry: a mechanism missing in current models to explain secondary inorganic aerosol formation during the January 2013 haze episode in North China, Atmos. Chem. Phys., 14, 2031-
785 2049, https://doi.org/10.5194/acp-15-2031-2015, 2015.

Zhou, C. H., Gong, S., Zhang, X. Y., Liu, H. L., Xue, M., Cao, G. L., An, X. Q., and Che, H. Z.: Towards the improvements of simulating the chemical and optical properties of Chinese aerosols using an online coupled model - CUACE/Aero, Chemical and physical and meteorology, https://doi.org/10.3402/tellusb.v64i0.18965, 2012.

Zhou, C. H., Zhang, X. Y., Gong, S., Wang, Y. Q., and Xue, M.: Improving aerosol interaction with clouds and precipitation in a regional chemical weather modeling system, Atmospheric Chemistry and Physics, 16, 145-160, https://doi.org/10.5194/acp-16-145-2016, 2016.

Zhou, S., Wu, L., Guo, J., Chen, W., Wang, X., Zhao, J., Cheng, Y., Huang, Z., Zhang, J., Sun, Y., Fu, P., Jia, S., Tao, J., Chen, Y., and Kuang, J.: Measurement report: Vertical distribution of atmospheric particulate matter within the urban boundary layer in southern China – size-segregated chemical composition and secondary formation through cloud processing and heterogeneous reactions, Atmos. Chem. Phys., 20, 6435-6453, https://doi.org/10.5194/acp-20-6435-2020, 2020.

Zhou Y., Gong S., Zhou C., Zhang L., He J., Wang Y., Ji D., Feng J., Mo J., Ke H..: A new parameterization of uptake coefficients for heterogeneous reactions on multi-component atmospheric aerosols, Science of the Total Environment, 781, https://doi.org/10.1016/j.scitotenv.2021.146372, 2021.

Zhu, Y., Yang, L., Chen, J., Kawamura, K., Sato, M., Tilgner, A., van Pinxteren, D., Chen, Y., Xue, L., Wang, X., Simpson, I. J., Herrmann, H., Blake, D. R., and Wang, W.: Molecular distributions of dicarboxylic acids, oxocarboxylic acids and α-dicarbonyls in $PM_{2.5}$ collected at the top of Mt. Tai, North China, during the wheat burning season of 2014, Atmos. Chem. Phys., 18, 10741-10758, https://doi.org/10.5194/acp-18-10741-2018, 2018.

(a) Case 1 (b) Case 2
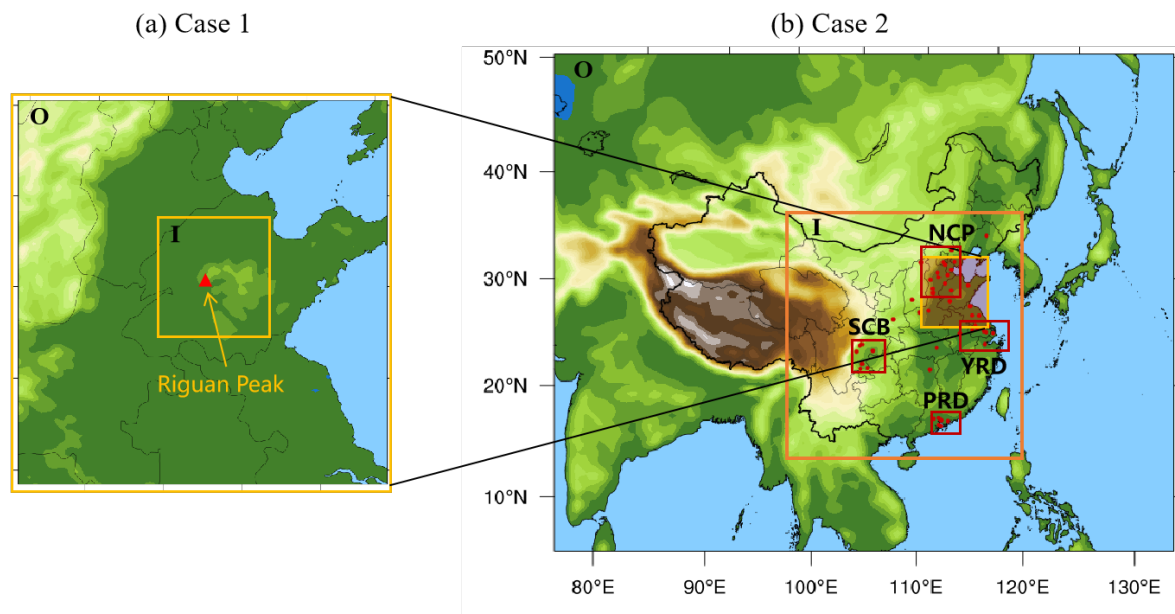
Figure 1. Model nesting domains and target regions. (a) domain for the Case 1. The red triangle is the Mount Tai observation site. (b) nesting domains for regional assessment for Case 2. Red dots are some cities where the surface observations of air pollutants are used for model evaluation. The target four regions are NCP for the North China Plain, YRD for the Yangtze River Delta, PRD for the Pearl River Delta and SCB for the Sichuan Basin.
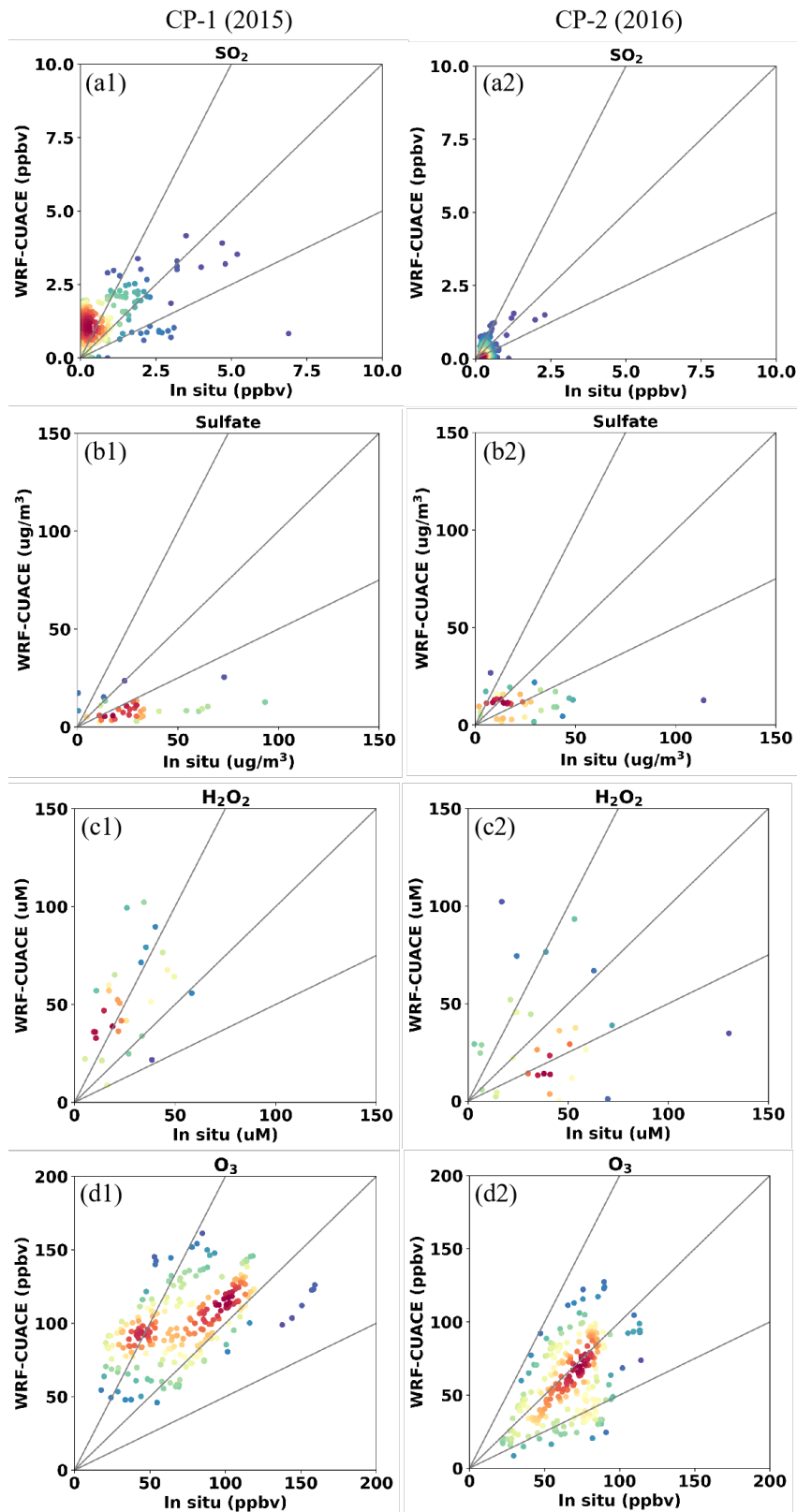
Figure 2. Scatter plots of hourly SO_2 (a1, a2), sulfate (b1, b2), H_2O_2 (c1, c2) and O_3 (d1, d2) concentrations between WRF/CUACE and in situ observations at Mount Tai in CP-1 and CP-2. Units: SO_2 and O_3 (ppbv), H_2O_2 (μM), and Sulfate (μg/m³). The color of the dots represents the density, and the red color is the high density area.
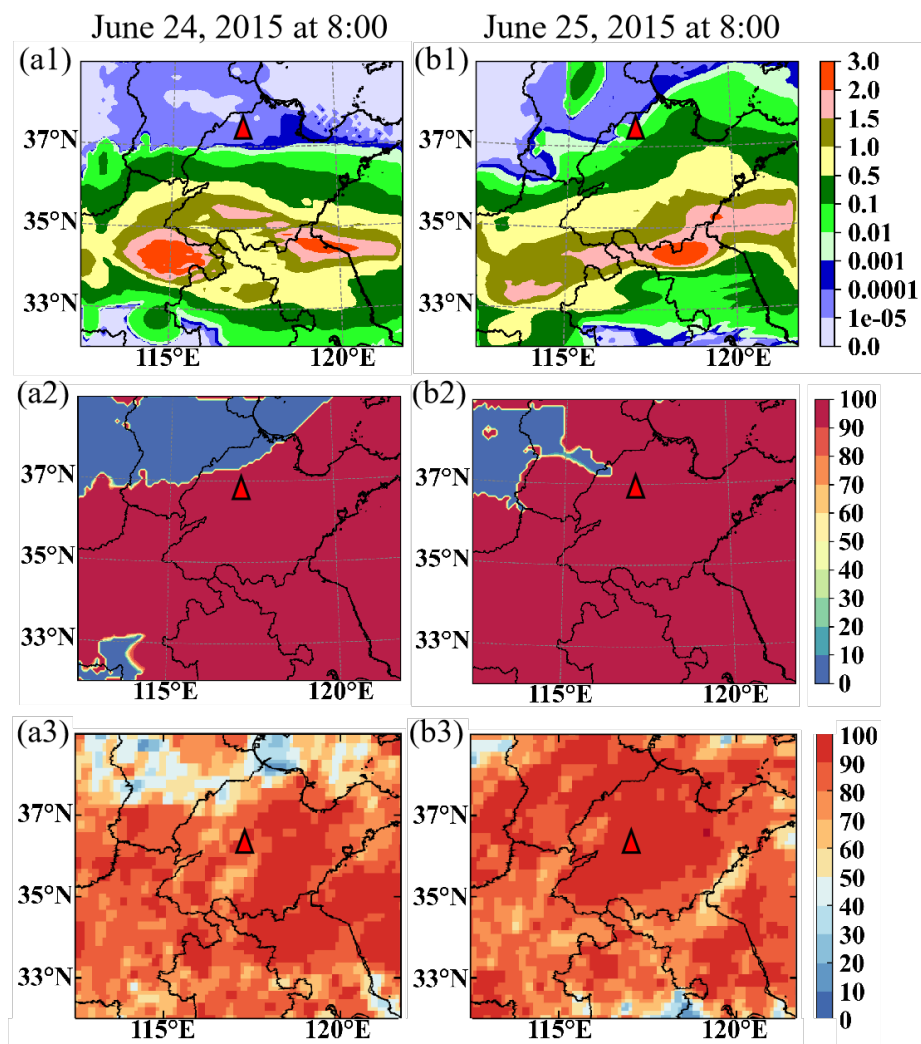
Figure 3. Cloud Water Simulation and Satellite Comparison. **The column liquid water content by WRF/CUACE (a1, b1, Units: kg/m^2), the cloud fraction by WRF/CUACE.(a2, b2, Units: %) and the cloud total amount of FY2G, (a3, b3, Units: %). (a) is for 8:00 LST on 24 June 2015, (b) is for 8:00 LST on 25 June 2015. The red triangle is the Mount Tai observation site.**
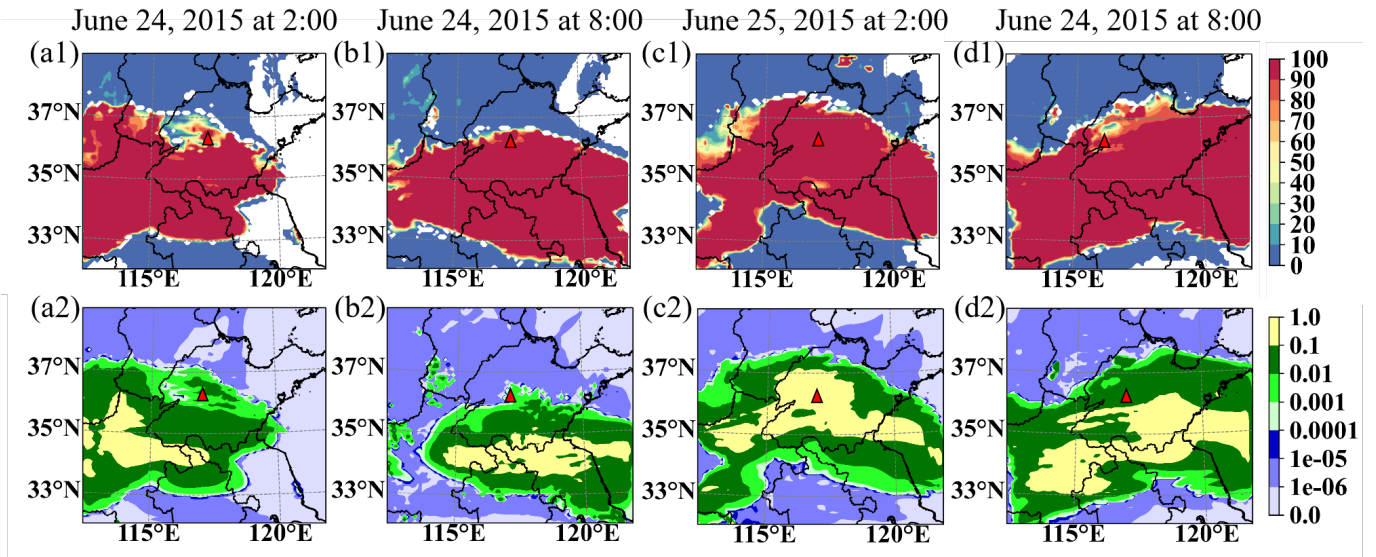
Figure 4. Regional comparison of intracloud SO₂ oxidation with cloud water at the high of Mount Tai. Distributions of SO₂ oxidation rate (a1, b1, c1 and d1, Units: %) and the liquid water content (a2, b2, c2 and d2, Units: g/kg) by WRF/CUACE, where (a) is for 2:00 LST on 24 June 2015, (b) is for 8:00 LST on 24 June 2015, (c) is for 2:00 LST on 25 June 2015 and (d) is for 8:00 LST on 25 June 2015. The red triangle is the Mount Tai observation site.
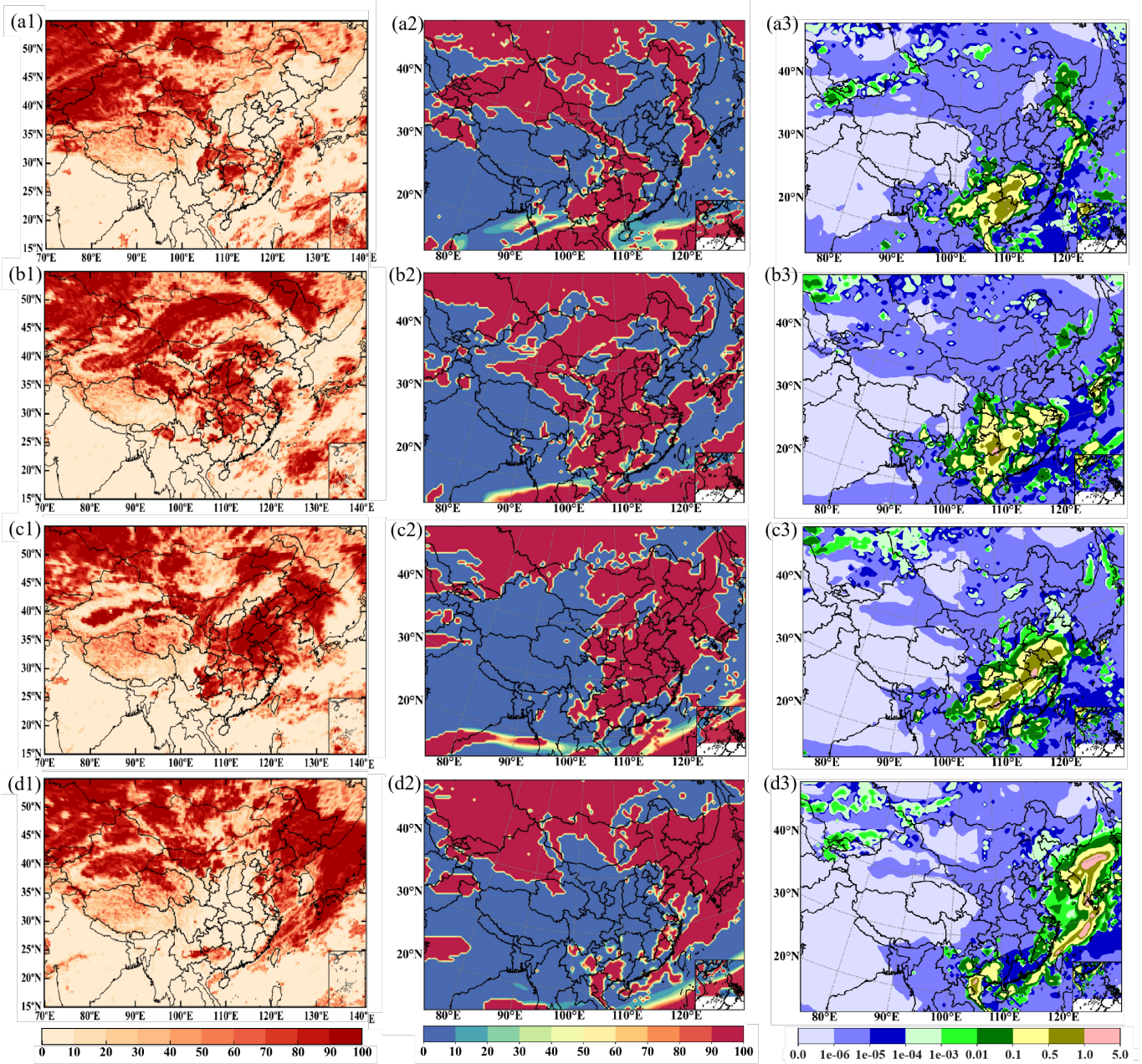
Figure 5. Cloud Water Simulation and Satellite Comparison in a heavy pollution episode. The cloud total amount of FY-2G (a1, b1, c1, d1, Units: %), the column cloud of WRF/CUACE (a2, b2, c2, d2, Units: %) and the column liquid water content of WRF/CUACE (a3, b3, c3, d3, Units: kg/m²). (a) is for 8:00 LST on 19 Dec., (b) is for 8:00 LST on 20 Dec., (c) is for 8:00 LST on 21 Dec., and (d) is for 8:00 LST on 22 Dec.
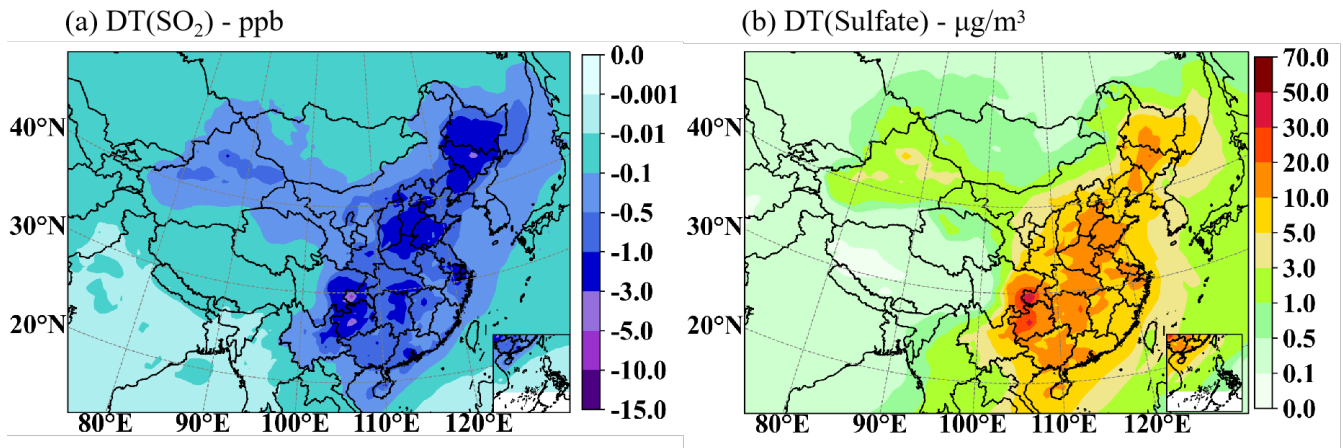
Figure 6. The mean SO₂ concentration decreased (a) and sulfate concentration increased (b) by cloud chemistry for DEC.
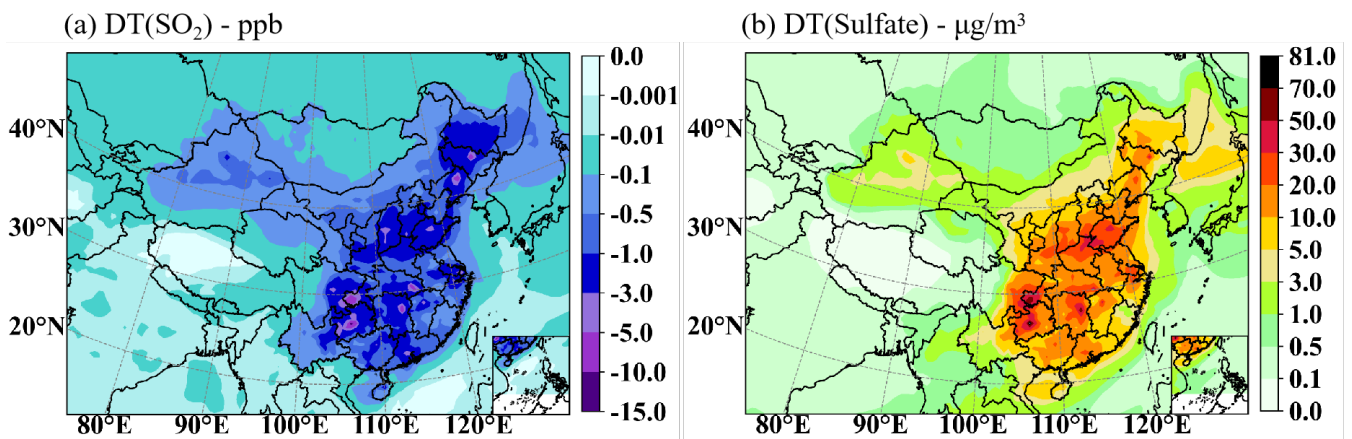
Figure 7. The mean SO₂ concentration decreased (a) and sulfate concentration increased (b) by cloud chemistry for HPE-2.
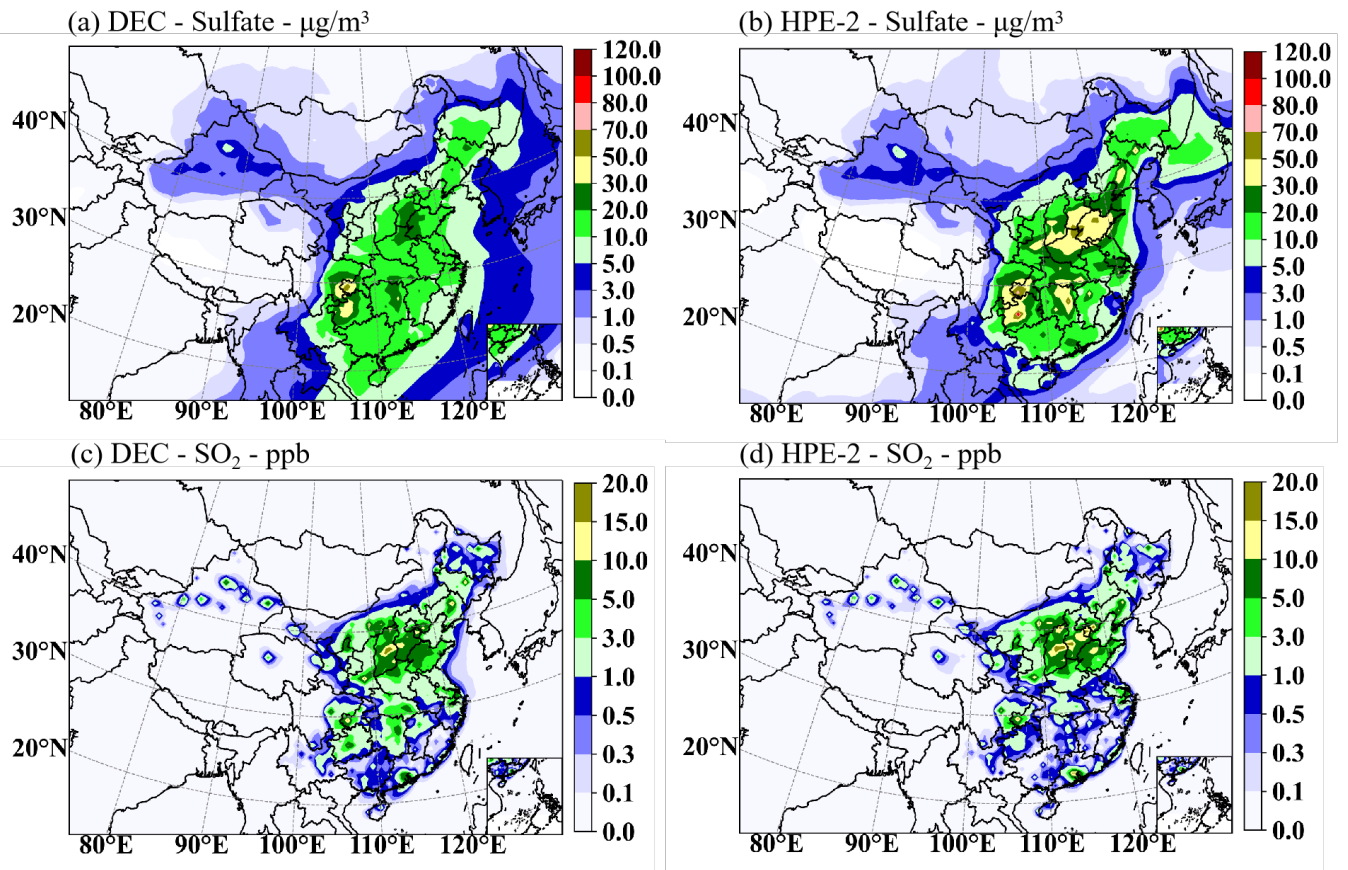
Figure 8. The mean sulfate concentration for DEC (a, c) and HPE-2 (b, d) for SO₂ (c, e) and sulfate (a, b).
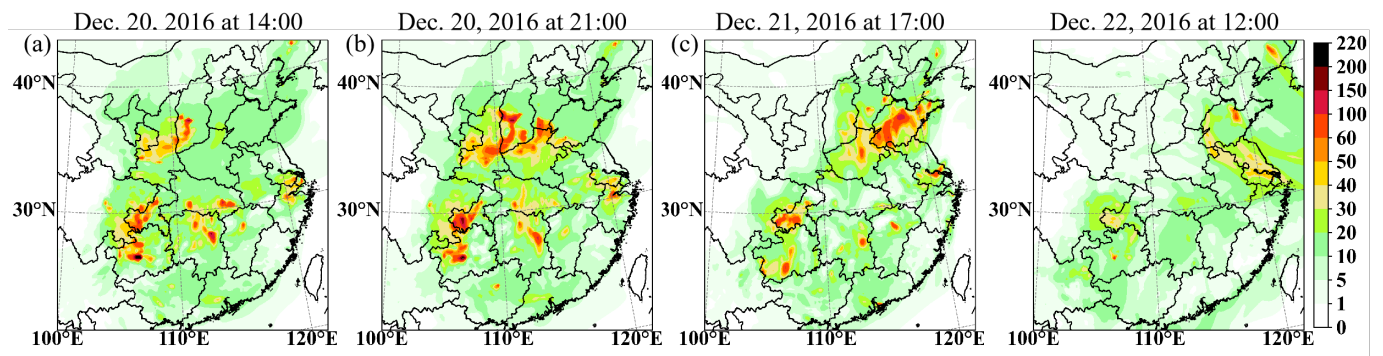
Figure 9. The differences in surface sulfate concentrations between with and without cloud chemistry at 21:00 LST on 20 Dec. (a), at 17:00 LST on 21 Dec. (b), and at 12:00 LST on 22 Dec. (c) (Units: μg/m³).
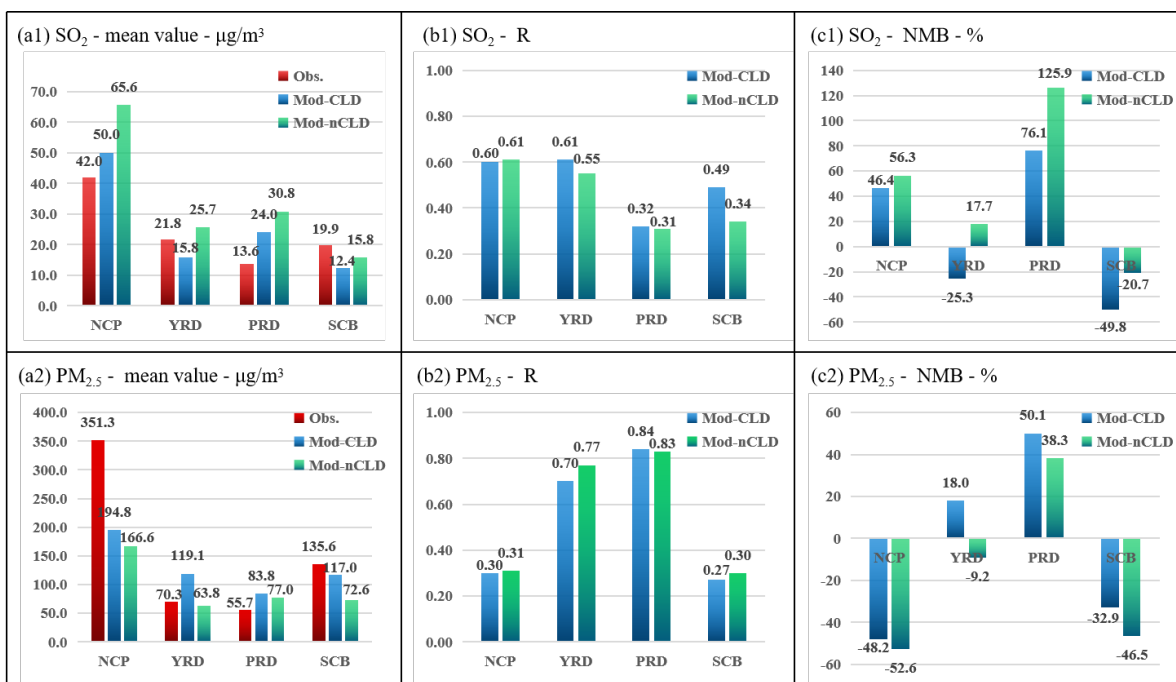
Figure 10. Statistical metrics for hourly SO₂ and PM₂.₅ for four regions for HPE-2 with (Mod-CLD) and without (Mod-nCLD) cloud chemistry. The mean value (a1, Units: μg/m³), R (b1) and NMB (c1, Units: %) of SO₂ as well as the mean value (a2, Units: μg/m³), R (b2) and NMB (c2, Units: %) of PM₂.₅. Obs. denotes the observations.
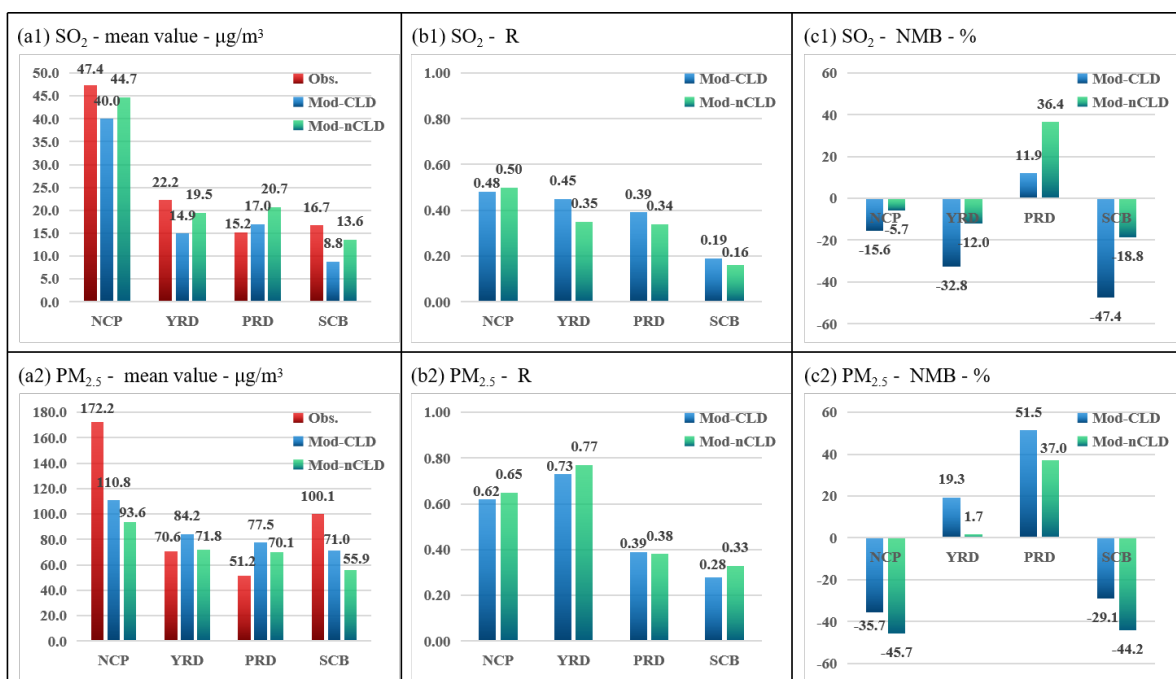
Figure 11. Statistical metrics for hourly SO₂ and PM₂.₅ for four regions for DEC with (Mod-CLD) and without (Mod-nCLD) cloud chemistry. The mean value (a1, Units: μg/m³), R (b1) and NMB (c1, Units: %) of SO₂ as well as the mean value (a2, Units: μg/m³), R (b2) and NMB (c2, Units: %) of PM₂.₅. Obs. denotes the observations.
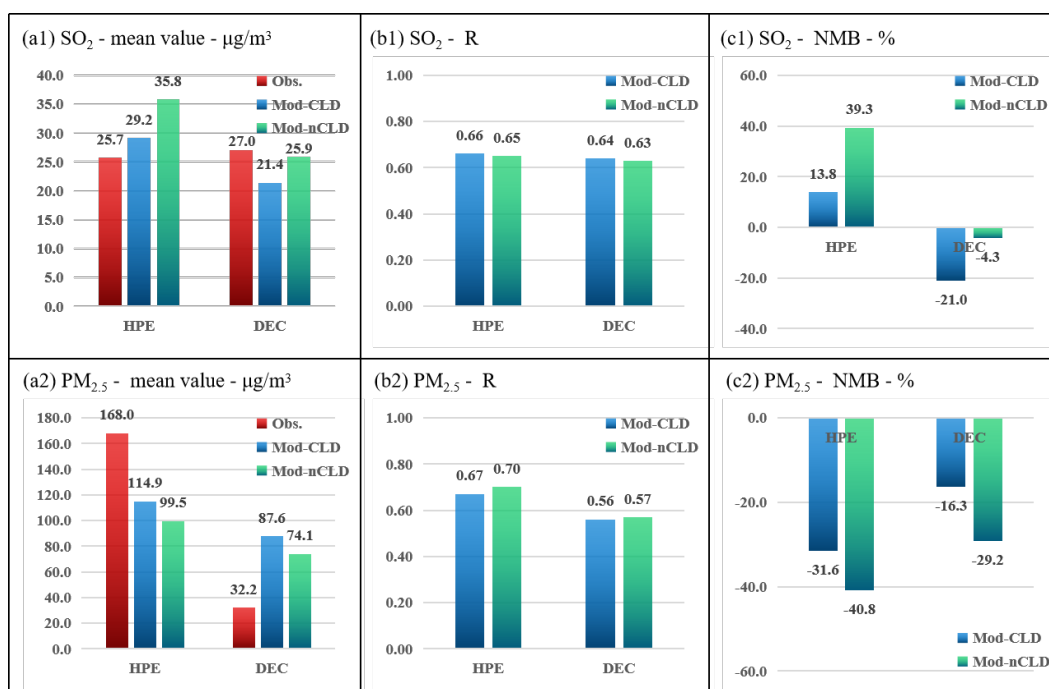
Figure 12. Statistical metrics for hourly SO₂ and PM₂.₅ in all selected sites for HPE-2 and DEC with (Mod-CLD) and without (Mod-nCLD) cloud chemistry. The mean value (a1, Units: μg/m³) , R (b1) and NMB (c1, Units: %) of SO₂ as well as the mean value (a2, Units: μg/m³) , R (b2) and NMB (c2, Units: %) of PM₂.₅. Obs. denotes the observations.
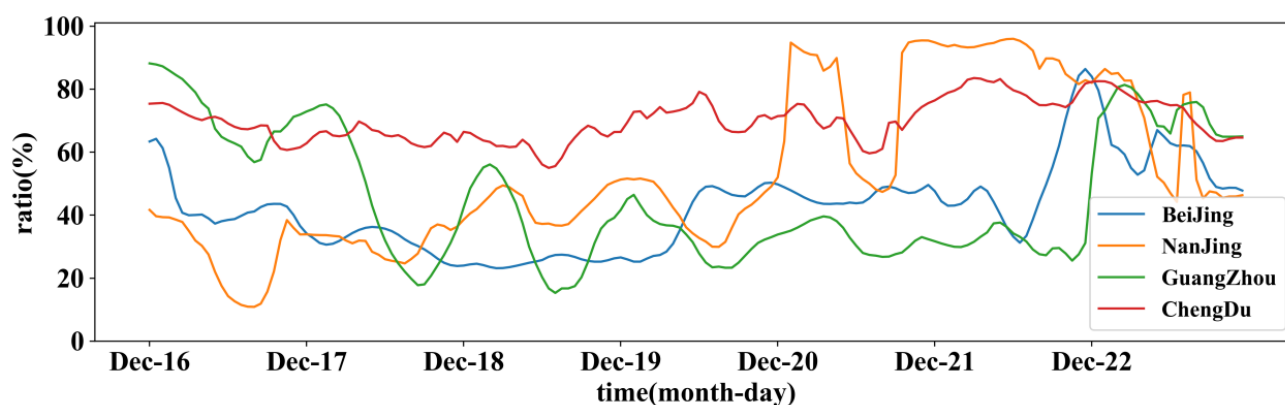
Figure 13. The rates of SO₂ column concentration reduced by cloud chemistry in Beijing (blue), Nanjing (yellow), Guangzhou (green) and Chengdu (red).
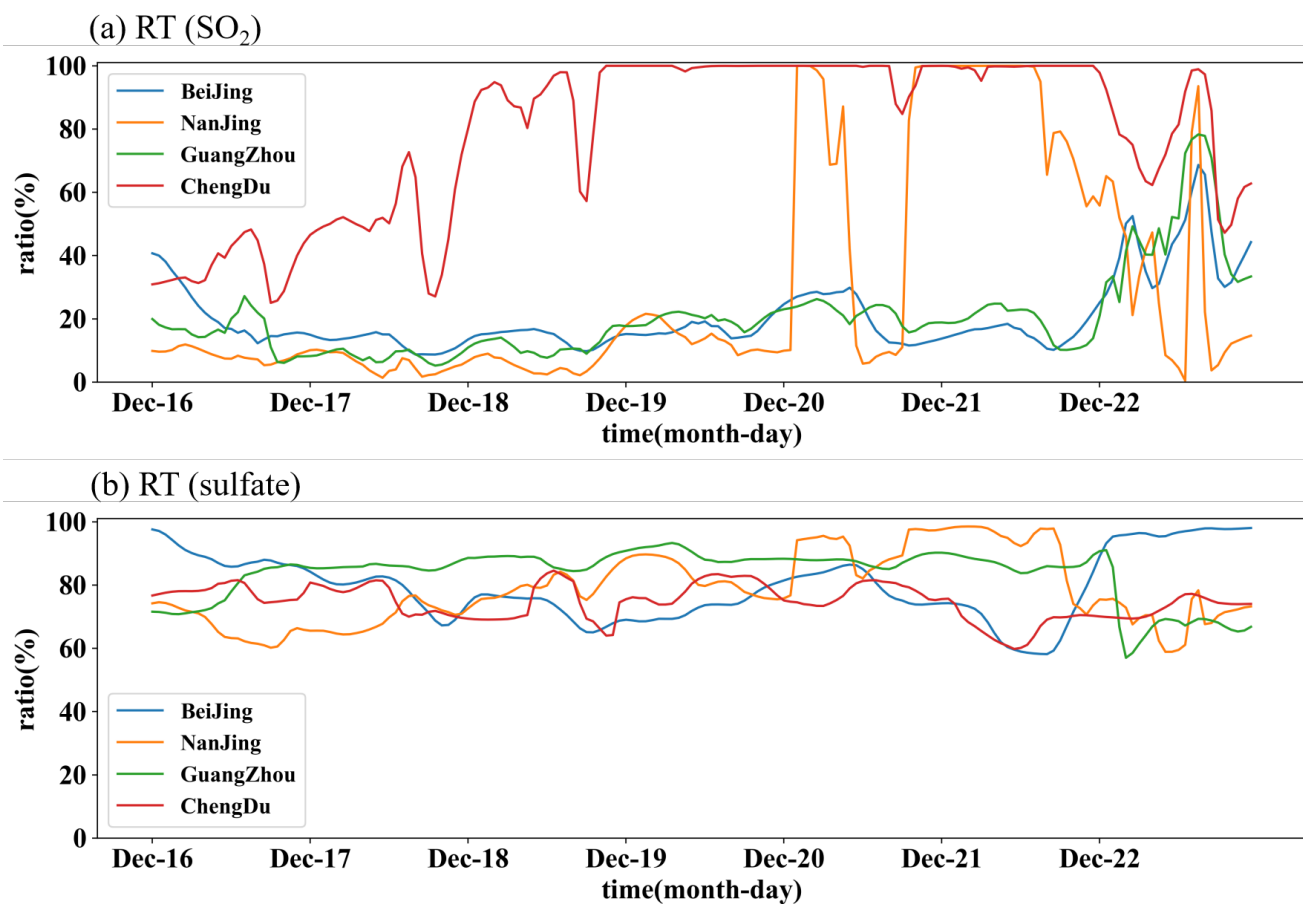
Figure 14. The rates of surface SO₂ reduced (a) and the surface sulfate increased (b) influenced by cloud chemistry in Beijing (blue), Nanjing (yellow), Guangzhou (green) and Chengdu (red).
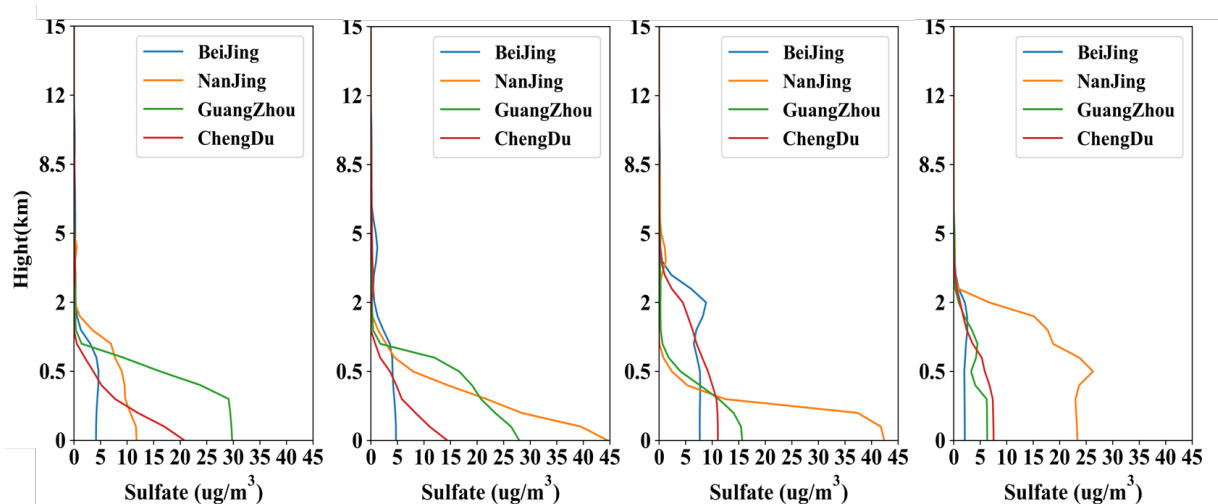
Figure 15. Vertical profiles of sulfate concentration difference (DT) at 12:00 on 20 Dec., at 21:00 on 20 Dec., at 17:00 on 21 Dec., and at 12:00 on 22 Dec. in Beijing (blue), Nanjing (yellow), Guangzhou (green) and Chengdu (red).

Table 1. Equilibrium Constants for the Parameterization of the Cloud Chemistry in CUACE.

Equilibrium Relation	Constant Expression	Equilibrium Constant		
		K(298)	a	Unit
$SO_2(g) + H_2O(aq) \leftrightarrow SO_2(aq)$	$K_{HS} = \dfrac{[SO_2(aq)]}{[SO_2(g)]}$	1.23	3120	$\dfrac{M}{atm}$
$SO_2(aq) \leftrightarrow H^+ + HSO_3^-$	$K_{1S} = \dfrac{[H^+][HSO_3^-]}{[SO_2(aq)]}$	1.7×10^{-2}	2090	M
$HSO_3^- \leftrightarrow H^+ + SO_3^{2-}$	$K_{2S} = \dfrac{[H^+][SO_3^{2-}]}{[HSO_3^-]}$	6.0×10^{-8}	1120	M
$O_3(g) + H_2O(aq) \leftrightarrow O_3(aq)$	$K_{HO} = \dfrac{[O_3(aq)]}{[O_3(g)]}$	1.15×10^{-2}	2560	$\dfrac{M}{atm}$
$H_2O_2(g) + H_2O(aq) \leftrightarrow H_2O_2(aq)$	$K_{HP} = \dfrac{[H_2O_2(aq)]}{[H_2O_2(g)]}$	9.7×10^4	6600	$\dfrac{M}{atm}$

Table 2. physics parameterization schemes in WRF.

Physical management	Parameterization	References
microphysics scheme	Lin	Lin et al. (1983)
shortwave radiation	Goddard	Chou and Suarez (1994)
longwave radiation	RRTM	Mlawer et al. (1997)
land surface scheme	Noah	Chen and Dudhia (2001)
boundary layer scheme	MYJ	Janjić (1994)
cumulus scheme	Grell-3D	Grell (1993)

Table 3. Statistics for SO₂, O₃, H₂O₂ and sulfate in cloud chemistry at Mount Tai site.

		Observed Mean	Simulated Mean	R	RAD (%)	NMB (%)
CP-1	SO_2	2.2	2.3	0.34	-3.4	7.1
	O_3	97.8	55.3	0.33	27.8	-43.5
	H_2O_2	26.5	16.8	0.78	22.4	-36.6
	Sulfate	31.7	9.2	0.32	55.0	-71.0
CP-2	SO_2	0.6	0.6	0.47	-6.1	12.9
	O_3	60.7	51.0	0.40	8.7	-16.0
	H_2O_2	46.9	32.4	0.06	18.4	-29.6
	Sulfate	28.1	11.4	0.54	42.2	-59.4

Note: unit of SO_2 and O_3 (ppbv), H_2O_2 (μM), and Sulfate (μg/m³)

Table 4. Statistical metrics for meteorology in four regions for HPE and DEC

		Observed Mean		Simulated Mean		R		NMB(%)		RMSE	
		HPE	DEC	HPE	DEC	HPE	DEC	HPE	DEC	HPE	DEC
N	T2	1.0	1.1	2.8	2.1	0.70	0.84	187.3	84.9	3.3	2.5
C	RH2	78.8	68.3	52.3	48.8	0.54	0.64	-33.7	-28.6	32.3	25.9
P	WS10	1.5	1.7	1.7	2.2	0.49	0.54	14.1	27.5	1.2	1.3
Y	T2	9.2	8.0	9.5	8.4	0.94	0.96	2.9	5.1	1.4	1.3
R	RH2	79.2	75.6	73.8	73.0	0.86	0.85	-6.8	-3.5	10.7	9.3
D	WS10	2.2	2.3	2.8	3.0	0.74	0.76	28.7	31.9	1.2	1.3
P	T2	18.3	17.3	19.0	17.9	0.93	0.92	3.6	3.8	1.9	1.9
R	RH2	72.2	70.4	64.3	65.4	0.76	0.68	-10.9	-7.2	14.0	13.9
D	WS10	1.8	2.4	2.0	3.2	0.67	0.72	13.6	37.1	1.0	1.5
S	T2	10.2	9.7	10.5	10.0	0.74	0.75	2.8	3.1	1.8	2.2
C	RH2	81.6	79.9	74.1	71.3	0.66	0.60	-9.2	-10.8	12.7	15.5
B	WS10	1.1	1.3	1.6	1.9	0.49	0.36	49.2	50.5	1.0	1.3

Note: unit of T2 (℃), RH2(%) and WS10 (m/s)

Table 5. Statistical metrics for hourly SO₂, O₃ and PM₂.₅ in four regions for HPE and DEC

		Observed Mean ($\mu g/m^3$)		Simulated Mean ($\mu g/m^3$)		R		NMB(%)	
		HPE	DEC	HPE	DEC	HPE	DEC	HPE	DEC
NCP	SO_2	42.0	61.5	50.0	40.0	0.60	0.48	46.3	-15.6
	O_3	8.8	7.4	7.4	10.9	0.47	0.60	-15.3	-32.4
	$PM_{2.5}$	351.3	182.1	194.8	110.8	0.30	0.62	-48.2	-35.7
YRD	SO_2	21.8	16.3	15.8	14.9	0.61	0.45	-25.3	-32.8
	O_3	31.3	14.4	9.3	22.1	0.33	0.68	-54.0	-45.5
	$PM_{2.5}$	70.3	82.9	119.1	84.2	0.70	0.73	18.0	19.3
PRD	SO_2	13.6	24.0	24.0	17.0	0.32	0.39	76.1	11.9
	O_3	45.7	56.3	56.5	57.4	0.84	0.80	23.0	13.9
	$PM_{2.5}$	55.7	83.6	83.8	77.5	0.84	0.39	50.1	51.5
SCB	SO_2	20.0	10.0	12.4	8.8	0.49	0.19	-49.8	-47.4
	O_3	22.0	49.0	45.3	54.2	0.20	0.47	123.1	97.4
	$PM_{2.5}$	135.6	91.0	117.0	71.0	0.27	0.28	-32.9	-29.1